



Cite this: *RSC Adv.*, 2021, **11**, 7187

Received 5th December 2020  
 Accepted 12th January 2021

DOI: 10.1039/d0ra10275  
[rsc.li/rsc-advances](http://rsc.li/rsc-advances)

## Magnetic aerogel: an advanced material of high importance

Nasrullah Shah, <sup>ab</sup> Touseef Rehan, <sup>c</sup> Xuemei Li, <sup>ad</sup> Halil Tetik, <sup>a</sup> Guang Yang, <sup>a</sup> Keren Zhao<sup>a</sup> and Dong Lin<sup>\*a</sup>

Magnetic materials have brought innovations in the field of advanced materials. Their incorporation in aerogels has certainly broadened their application area. Magnetic aerogels can be used for various purposes from adsorbents to developing electromagnetic interference shielding and microwave absorbing materials, high-level diagnostic tools, therapeutic systems, and so on. Considering the final use and cost, these can be fabricated from a variety of materials using different approaches. To date, several studies have been published reporting the fabrication and uses of magnetic aerogels. However, to our knowledge, there is no review that specifically focuses only on magnetic aerogels, so we attempted to overview the main developments in this field and ended our study with the conclusion that magnetic aerogels are one of the emerging and futuristic advanced materials with the potential to offer multiple applications of high value.

<sup>a</sup>Department of Industrial and Manufacturing Systems Engineering, Kansas State University, Manhattan, KS 66506, USA. E-mail: [dongl@ksu.edu](mailto:dongl@ksu.edu); [nasrchem@gmail.com](mailto:nasrchem@gmail.com); Tel: +1-785-2372200; +1-785-4911492

<sup>b</sup>Department of Chemistry, Abdul Wali Khan University Mardan, Mardan, KP 23200, Pakistan

<sup>c</sup>Department of Biochemistry, Quaid-i-Azam University, Islamabad 24000, Pakistan

<sup>d</sup>Key Laboratory of High Efficiency and Clean Mechanical Engineering, Shandong University, Jinan 250061, China



Dr Nasrullah Shah is A/ Professor at the Abdul Wali Khan University Mardan (AWKUM), Pakistan, and doing research as the Fulbright Scholar at the Kansas State University, USA. Dr Shah holds a PhD degree in Chemical Engineering from KNU, Korea. He has post-doctoral experience at the University of Sheffield, UK. Dr Shah has vast experience in the field of fabrication, characterization, and applications of advanced materials. He has published several research publications in reputed international journals with 1031 citations. Dr Shah has expertise in additive based composite materials for biomedical, environmental, and analytical applications. Recently, he is working in additive manufacturing (3D printing) based materials projects, and has also submitted papers for publication in this field. Dr Shah has received several awards including the KNU Honor scholarship for PhD, AWKUM merit scholarship for post-doc. The Fulbright award for post-doc, and three research grants from HEC, Pakistan.



Dr Dong Lin is serving as A/ Professor at the department of industrial and manufacturing systems engineering, Kansas State University. Dr Lin qualification brief is MS in Industrial Engineering from University of Nebraska Lincoln, USA, PhD in Industrial Engineering, from Purdue University, USA. Dr Lin is an expert in the manufacturing of aerogels. Lin's most recent research interests focus on 3D printing of multifunctional aerogels for various applications, and 3D printing of carbon fiber composites. He has one Guinness World Record with his collaborators: The World's lightest material via 3D printing. Dr Lin has 62 publications in reputed international journals with a total impact factor of 2184. Dr Lin was awarded the Big 12 Faculty Fellowship in 2016. While at Purdue University, Lin was awarded the Ross Fellowship, a four-year package to recruit outstanding PhD track students, from 2009 to 2013. He was a member of Tau Beta Pi Engineering Honor Society at the University of Nebraska Lincoln in 2008. He received the Siemens Scholarship from the Siemens Foundation in 2007.



## 1. Introduction

S. S. Kistler used the hypothesis of replacing the liquid of hydrogel with gas to obtain a porous material with no to little shrinkage and he succeeded in preparing the first silica aerogel by first making its gel followed by solvent exchange and finally drying in an autoclave. In the same work, Kistler reported the synthesis of aerogels from several other materials.<sup>1</sup> This was followed by several patents of aerogels including five US patents of Kistler himself and a few others from other researchers.<sup>2</sup> Further research was stuck until the work of Cantin *et al.* who reported a simplified process of making silica aerogel by removing methanol from silica alcogel in an autoclave without using a multiple solvents exchange process.<sup>3</sup> This was followed by enormous work to bring improvements in the synthesis methods, compositions, properties, and performance of aerogels.<sup>4-12</sup>

Aerogels have the unique properties of having the least density, high porosity, large surface area, and high capacity of accommodating other materials within their matrix which make them applicable in diverse fields.<sup>6,13,14</sup>

The preparation of nanocomposites is in focus due to the fact that their properties can be tuned by changing the composition and size of the incorporated nanoparticles.<sup>15-17</sup> Nanoparticles as additives have specific properties that greatly influence the electronic, optical, catalytic, and magnetic properties of the composites.<sup>15,18,19</sup>

The incorporation of magnetic materials in aerogels by various methods shown in Fig. 1, opens up fascinating possibilities for applications in several fields like environmental remediation, catalysis, magnetic field-assisted chemical reactions, controlled drug delivery applications, microwave absorption, electromagnetic interference (EMI) shielding, radiotherapy, catalysis, magnetic high-density storage devices, and devising therapeutic and sensing types of equipment.<sup>20-29</sup> The use of different types of drying techniques are done in order

to achieve aerogels of the desired characteristics as it has also been reported for cryogels that the drying processes are noted to have a great effect on the final morphological, structural and physical characteristics of the materials.<sup>30</sup> The microwave absorption capability, drug delivery application, catalytic ability, mechanical properties, and re-usability of the pristine aerogels can be improved by making their composites.<sup>29,31-33</sup>

Some of the important application areas of the magnetic aerogel are shown in Fig. 2.

This is due to the fact that the nanocomposites formed by the combination of nanoparticles as additives with the porous structures greatly impact the magnetic, electronic, and other characteristics of the final materials that are used for attaining numerous application areas.<sup>34</sup>  $\text{Fe}_3\text{O}_4$  nanoparticles provide superparamagnetic property to the materials and as a result widen their applications.<sup>35,36</sup> The  $\text{Fe}_3\text{O}_4$  nanoparticles also show interaction to water molecules without changing their structures that causes a change in the final electrical property of the materials.<sup>37,38</sup> The same is true for other particles such as iron-cobalt alloys, metal ferrite, iron, iron carbides, and superparamagnetic metallic particles, *etc.* that induce magnetic property to the composite aerogel materials.<sup>31,39-42</sup> Based on the present study, it can be interpreted that according to the type of matrix materials of the magnetic aerogels the mostly reported magnetic aerogels are with silica matrix followed by carbon, natural-polymers/ cellulose, metals, synthetic polymers, alumina and clays as represented by a pie diagram in Fig. 3.

Furthermore, as far as our knowledge is concerned, to date, there is no specific review regarding magnetic aerogel, hence, keeping in mind the importance of magnetic aerogels this study is designed to encircle the major developments related to this futuristic advanced material. This review is focused on classifying the magnetic aerogels based on the composition of major matrix materials along with some information on their preparation methods and uses, to pave a way for future research.

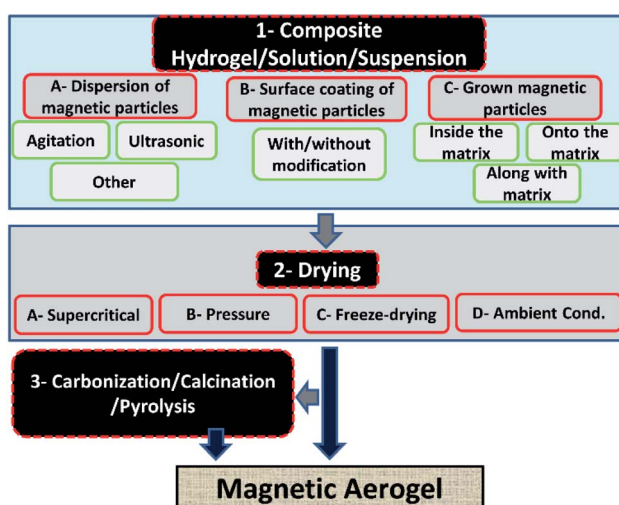


Fig. 1 Generalized and broader classification of fabrication methods of magnetic aerogels.

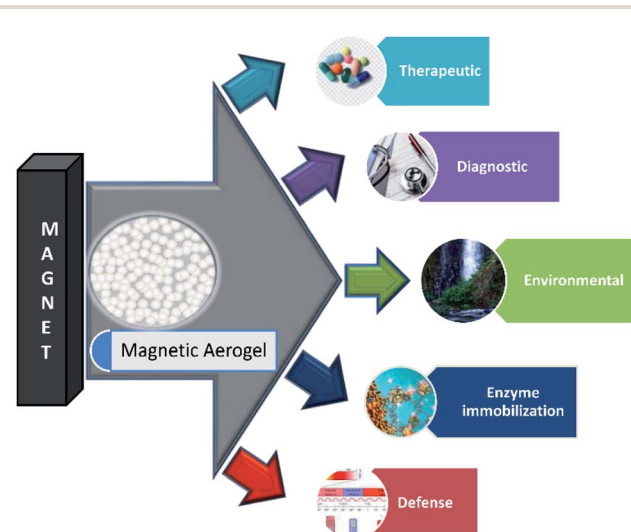


Fig. 2 Various potential application areas of magnetic aerogels.



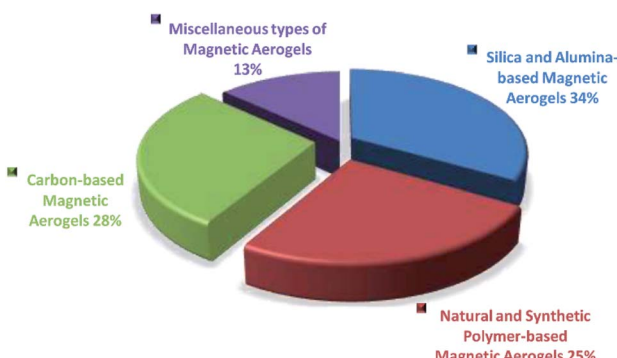


Fig. 3 Considering the literature survey in the present study, the distribution of magnetic aerogels on the basis of major types.

## 2. Silica and alumina-based magnetic aerogels

Silica aerogels are known for having highly inert nature and used for various purposes with a predominant use as insulator and adsorbent.<sup>9,33,43</sup> Their composites form made them more versatile in applications.<sup>44,45</sup> Introducing magnetic property into the silica aerogels has increased their performance as a catalyst, adsorbent, sensor, drug delivery agents, enzyme immobilization, EMI shielding *etc.* Magnetic property is introduced by using different approaches to combine magnetic materials with aerogel matrix for obtaining silica and alumina-based magnetic aerogels. For this purpose, the use of magnetite nanoparticles is broadly studied. However, some other magnetic additives have also been incorporated for obtaining silica and alumina-based magnetic aerogels. The studies of fabrication of alumina-based magnetic aerogels are limited compared to silica-based magnetic aerogels.

Magnetic iron oxide/silica aerogel with mesoporous structure and high surface area (max.  $411 \text{ m}^2 \text{ g}^{-1}$ ) was prepared by the sol-gel process followed by simply drying at  $80\text{--}150^\circ\text{C}$  and was successfully used for Rhodamine B adsorption. The adsorbent showed 95.8% adsorption within 80 min and was easily recoverable from aqueous solution through a magnet. The effect of ultrasonication was found favorable for getting a uniform porous structure with a high surface area.<sup>32</sup> The aerosol iron was first prepared by fast evaporation of iron-pentacarbonyl from tungsten filament in inert atmosphere followed by coating oxide layer on their surface by chemical treatment and then was utilized in synthesizing core-shell particles. The core-shell particles were dispersed in silica matrix for getting a magnetically active nanocomposite aerogel. A simple sol-gel/supercritical drying process was followed for preparing the aerogel and the resultant magnetic composite aerogel. They correlated the magnetic property of the as-prepared magnetic aerogel to the Fe powder and found a direct relation. The obtained magnetic aerogel had very low density ( $110 \text{ mg cm}^{-3}$ ), high surface area ( $650 \text{ m}^2 \text{ g}^{-1}$ ) and a suitable saturation magnetization value ( $\sim 6.4 \text{ emu g}^{-1}$ ).<sup>34</sup> Silica-based composite magnetic aerogel was prepared by

ambient pressure drying method by introducing magnetic iron oxide particles and other additives in the sol-gel process for use in the wastewater treatment process. The obtained lightweight (density of  $106 \text{ mg cm}^{-3}$ ) magnetic aerogel had a high surface area ( $695 \text{ m}^2 \text{ g}^{-1}$ ) and low thermal conduction ( $0.029 \text{ W m}^{-1} \text{ K}$ ) that make them able for multiple applications. The environmental application was checked by using them for adsorption of organic solvents and obtained an adsorption capacity of  $191.8 \text{ mg/18.4 mg}$  of aerogel. The magnetic ability was found suitable in easy recovery.<sup>46</sup> Aeromagnets with programmed magnetization ( $M \sim 380 \text{ A m}^{-1}$ ) were prepared by dispersing ferromagnetic nanorods/nanoplatelets in silica/nanocellulose matrix for use as actuators in robots. Due to well dispersion and orientation arrangement of magnetic additives, the resultant aeromagnet maintained high elasticity with stress-strain values of  $\sim 50 \text{ kPa}$  and 30% strain after several programmed magnetic cycles. The density was  $120 \text{ mg cm}^{-3}$  with a 70% porosity.<sup>47</sup> Considering the hyperthermia therapy application of magnetic particles, their dispersion was done into the silica matrix followed by treatment under a magnetic field to study the temperature increase. After application of  $560 \text{ Oe}$  of the magnetic field, the temperature of  $45^\circ\text{C}$  was achieved. The maximum saturation magnetization of  $17 \text{ emu g}^{-1}$  was reported for the respective aerogel. This silica-based magnetic aerogel was also recommended for drug delivery and other potential applications as well.<sup>48</sup> Amirkhani *et al.* reported silica-based magnetic aerogel by the sol-gel process (as illustrated in Fig. 4) using magnetic nanoparticles of iron oxide and sodium silicate precursors. For this purpose, they first prepared the hydrogel and immersed it into the iron oxide nanoparticles solution followed by drying. The prepared magnetic aerogel (density  $340 \text{ mg cm}^{-3}$ , surface area  $520 \text{ m}^2 \text{ g}^{-1}$ , and saturation

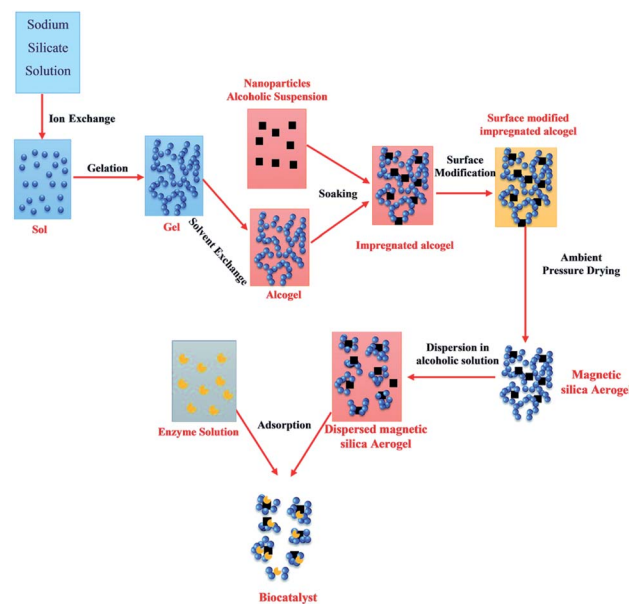


Fig. 4 Schematic representation of the synthetic procedure of biocatalyst. This figure has been adapted/reproduced from ref. 49 with permission from Royal Society of Chemistry, copyright 2020.



magnetization  $6.16 \text{ emu g}^{-1}$ ) was used as an adsorbent for the immobilization of *Candida rugosa* lipase. The enzyme activity studies were also performed. They found that the dispersed support magnetic aerogel particles produced good results for immobilization and activity compared to the dispersed one.<sup>49</sup>

Iron oxide microparticles were dispersed in the silica gel by application of the external magnetic field followed by supercritical drying to achieve a mesoporous magnetic composite aerogel with properly organized magnetic particles and possessed a density of  $250 \text{ mg cm}^{-3}$  and a high surface area ( $853 \text{ m}^2 \text{ g}^{-1}$ ) and magnetic ability. These aerogels were proposed for potential application as scaffolds for biomolecules and for tissue engineering.<sup>50</sup> Magnetic silica aerogels (magnetic susceptibility  $0.0025 \text{ emu g}^{-1} \text{ Oe}$ ) was synthesized by dispersing iron oxide nanoparticles in silica matrix by the sol-gel process followed by supercritical drying of the prepared gel. The high magnetic property and good dispersion of the magnetic particles were considered better for achieving better results. This study was focused on theoretical concepts but it can be helpful in understanding the background of the related studies.<sup>51</sup> Silica composite aerogels consisting of dispersed 1D and 2D additives were prepared for application in different areas including biomedical, electronic, storage, and catalytic applications.<sup>52</sup>

An attempt was made to produce magnetic aerogel by chemically crosslinking silica precursor in the presence of magnetic iron oxide particles. For getting better results the surfaces of the magnetic particles were chemically modified using an active silylation agent. The schematics of the synthesis process of this aerogel is given in Fig. 5. The low density ( $240 \text{ mg cm}^{-3}$ ) high magnetic ability (saturation magnetization  $54 \text{ emu g}^{-1}$ ) of the resultant silica-based aerogel along with improved mechanical strength (780 kPa), low thermal conductivity ( $0.055 \text{ W m}^{-1} \text{ K}$ ) and suitable surface area ( $53 \text{ m}^2 \text{ g}^{-1}$ ) make them suitable for potential in environmental cleaning as well as drug loading and delivery applications.<sup>53</sup>

The effect of different parameters on the magnetic behavior of hydrophobic magnetic aerogels was overviewed by Nagappan and Ha. It was concluded that the calcination temperature, composition, and some other parameters greatly affect the size and magnetic property of the final aerogel material.<sup>54</sup>

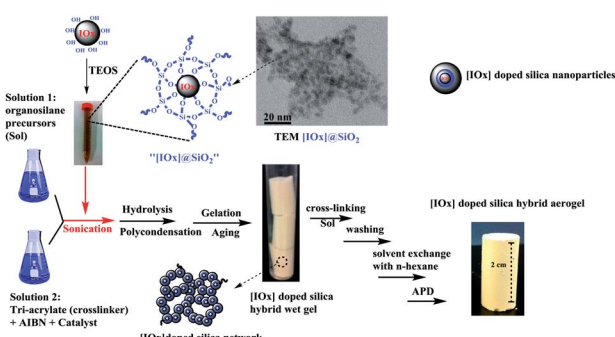


Fig. 5 Schematic synthesis steps for  $[\text{IOx}]$  doped hybrid silica aerogels. This figure has been adapted/reproduced from ref. 53 with permission from Elsevier under the license number 4957780788139, copyright 2020.

Maghemite-based silica hydrophobic aerogel composite was prepared from iron and silica precursors by sol-gel method followed by supercritical solvent extraction. The obtained magnetic aerogel was having a high surface area, mesoporosity (mean pore diameter of  $\sim 5 \text{ nm}$ ), and paramagnetic behavior with a maximum saturation magnetization value of  $0.6\text{--}1.7 \text{ emu g}^{-1}$  which make it suitable for adsorption and some other applications.<sup>55</sup> The effect of magnetic interparticle interactions on the magnetic properties of the maghemite silica aerogel composite was investigated by incorporating magnetic particles of about 5 nm sizes into the silica matrix. Different analytical techniques were used for the evaluation of the effect. The surface density of the absorber used in the magnetic measurement was in the range of  $50\text{--}80 \text{ mg cm}^{-2}$ . The maximum saturation magnetization value of  $24.8 \text{ emu g}^{-1}$  showed high paramagnetic behavior of the reported magnetic aerogel.<sup>56</sup> Silica composite incorporated with maghemite nanoparticles using the sol-gel preparation method. The effect of different drying conditions was evaluated for getting silica composite aerogel with high porosity, mechanical stability, and magnetic properties ( $0.3 \text{ emu g}^{-1}$ ) for various potential applications.<sup>57</sup> Luo *et al.* incorporated iron in the silica aerogel during its synthesis. Several aspects were studied such as they compared the physical properties of the prepared iron-based aerogel with surface-modified silica aerogels. They found that as prepared iron silica aerogel showed paramagnetic behavior with high hydrophobicity even at high temperature. However, shrinkage in porosity was also observed after the drying step. The obtained magnetic aerogel was having a low density ( $0.55\text{--}0.62 \text{ mg cm}^{-3}$ ), high surface area in the range  $798\text{--}956.8 \text{ m}^2 \text{ g}^{-1}$ , and porosity in the range of 74–76%. The saturation magnetization was not provided while the maximum magnetization moment value was  $\sim 0.07 \text{ emu g}^{-1}$ .<sup>58</sup> Magnetic silica aerogel composite was successfully synthesized by impregnating the silica gel with iron oxide precursors followed by supercritical drying. The resultant aerogel exhibited a large surface area ( $915 \text{ m}^2 \text{ g}^{-1}$ ), and mechanical stability (data not given) while maintaining the magnetic property ( $M_s \sim 11 \text{ emu g}^{-1}$ ) as well.<sup>59</sup> Silica-based magnetic aerogel composite was prepared by using two different approaches. In one approach the iron nitrate solution was used as a medium for gel polymerization of silica precursor and in another approach, the iron precursor solution was added to the already prepared silica. Both methods involved the drying of the prepared hydrogel by using the hypercritical solvent evaporation method. It was deduced from the experimental results that the magnetic property ( $M_s \sim 6 \text{ emu g}^{-1}$ ) of the final product can be controlled by varying various experimental conditions such as the composition of the ingredient and heating process involved in the whole process of fabrication of magnetic aerogels.<sup>60</sup>

Spinel structure zinc ferrite nanoparticles were dispersed in the porous silica aerogel and the change in the degree of inversion was noticed in ferrite nanoparticles within the aerogel matrix. They found that the degree of inversion increased with a decrease in particle size. The incorporation of ferrite nanoparticles provides the aerogel with magnetic properties ( $M_s \sim 6.4 \text{ emu g}^{-1}$ ) and the resultant magnetic aerogel. Furthermore,



the confinement of ferrite particle agglomerates in the porous structures of silica also enhanced the thermal fluctuation effect.<sup>61</sup> In an attempt to prepare cobalt ferrite silica aerogel composite with superparamagnetic behavior different amounts of cobalt ferrite were added to the silica matrix. The effect of composition and calcination temperature on the final properties of the prepared aerogel material was investigated and found superparamagnetic property increased with increase in ferrite amount and calcination temperature.<sup>17</sup> An interesting study was performed to check the role of temperature on the magnetic property of xerogel and aerogel of cobalt ferrite crystallite based silica aerogel composites. It was found that the magnetic properties of xerogel reduced with an increase in temperature but that of aerogel composite remained superparamagnetic even at 1100 °C. The reported aerogel was having surface area of 86 m<sup>2</sup> g<sup>-1</sup> with a maximum saturation magnetization value of ~19 emu g<sup>-1</sup>. Furthermore, it was also concluded from the study that other factors such as crystallite size, composition, and synthesis conditions also play a role in controlling the magnetic property of the final aerogel composite.<sup>62</sup>

Carta *et al.* studied the concomitant effect was observed by iron with Co or iron with Ni. The Ni and Co ferrite silica aerogel was synthesized and the effects of composition on the structural and magnetic properties of the aerogel were studied. It was found that the presence of ferrihydrite and diffusion of iron in the silicate hydroxide greatly influenced the magnetic property.<sup>40</sup> In another study by Carta *et al.*, the effect of high temperature on the porosity and formation mechanism was reported. The mesoporous cobalt ferrite silica composite aerogel was prepared and characterized by using different analytical techniques.<sup>63</sup> For high conversion of CO to methane gas NiCo additive based silica aerogel with a low density (80 mg cm<sup>-3</sup>), the high surface area of 201.2 m<sup>2</sup> g<sup>-1</sup>, and maximum saturation value of ~20 emu g<sup>-1</sup> was produced and used in the magnetic fluidized bed reactor.<sup>24</sup> FeCo alloy nanoparticles are reported for drug delivery, radiotherapy, diagnostic applications. The incorporation of these particles into aerogels have resulted in magnetic materials of improved properties and applications. In this study, the effect of alloy content on the incorporated particles size was also studied and concluded that the increase in FeCo alloy results in a decrease in particle size.<sup>64</sup>

Using the sol-gel approach FeCo alloy with different compositions of Fe : Co was dispersed in silica aerogel. The experiment was performed in acidic and basic conditions to know the effect of experimental conditions on the porosity of the composite aerogel. They found that the aerogels composite prepared at basic conditions were highly porous than that of prepared at acidic conditions. The magnetic property was also noticed to be influenced by the composition and experimental conditions. The maximum saturation magnetization value of the obtained aerogel was 11.5 emu g<sup>-1</sup>.<sup>39</sup> FeCo-SiO<sub>2</sub> composite aerogels with magnetic properties were fabricated by first preparing alcogel followed by supercritical drying while using iron nitrate, cobalt nitrate, and tetraethoxysilane as precursors. They also studied the effect of change in supercritical drying on the porosity of the prepared nanocomposite aerogel.<sup>65</sup> It is well reported that the magnetic property of the ferrite nanoparticles

is dependent on the cation distribution in the structure as well as the size of the particles. Zinc ferrite nanoparticle incorporated silica aerogel was prepared and characterized for structural and magnetic properties. It was found that there is a correlation between the particle size and particle interactions with the temperature for superparamagnetic transition and anisotropic constant. The decrease in anisotropic constant was more for smaller particles than on large particles for magnetic property of the resultant aerogel material. It was further elaborated that the inversion degree of the incorporated magnetic particles also contributed to the net magnetic property of the resultant aerogel composite.<sup>66</sup>

Silica gel was prepared and impregnated with an anhydrous iron(II) acetylacetone salt followed by supercritical drying to obtain the magnetic silica aerogel composite with a low density (200 mg cm<sup>-3</sup>), high surface area (774 m<sup>2</sup> g<sup>-1</sup>), and magnetic properties ( $M_s \sim 11$  emu g<sup>-1</sup>).<sup>67</sup> Silica magnetic iron oxide aerogel composite was synthesized by reacting salts of iron in the aerogel porous network acted as nanoreactors. The reported magnetic aerogel was having a low density (210–510 mg cm<sup>-3</sup>), high surface area (212–619 m<sup>2</sup> g<sup>-1</sup>), porosity (60–90%), and magnetic properties ( $M_s$  14 emu g<sup>-1</sup>). In this study, it was found that iron oxide phase, crystalline size, and the matrix structure are easy to change by varying the synthesis methods that can greatly change the final characteristics of the obtained aerogel. The purpose was achieving a material for magneto-optic sensors and magnetic devices.<sup>44</sup>

An interesting study of the use of silica-based aerogel magnetic composite for the capture of hypervelocity microparticles was performed. It was found that during the capture process the kinetic energy of the components transform into thermal energy which decreases or even diminishes the magnetic behavior of the magnetic particles.<sup>68</sup>

Various studies also reported the alumina-based magnetic aerogels for separation and catalytic purposes. Alumina based magnetic aerogel was synthesized for the removal of fluoride from water. The prepared magnetic alumina aerogel was reported to have high surface area (215.1 m<sup>2</sup> g<sup>-1</sup>), mesomacroporous nature, and a very high super magnetic nature (198 emu g<sup>-1</sup>) which made it suitable and a reusable adsorbent for fluoride separation. It showed an adsorption capacity of 32.1 mg of F<sup>-</sup> per gram.<sup>69</sup> FeCo alloy nanoparticles-based alumina aerogel composite was prepared by multiple-step process involving making a hydrogel by the sol-gel method, followed by supercritical drying and calcination. The saturation magnetization value of the aerogel changed with variation in temperature and time. The maximum saturation magnetization (~17 emu g<sup>-1</sup>) was observed at 700 °C. The correlation of the microstructure with the magnetic behavior of the composite aerogel was studied. It was found that the magnetic property is dependent on the composition of the nanoparticle and the interface of the particles with the alumina matrix.<sup>70</sup> Alumina nanocomposite aerogel was prepared by combining the precursor chemicals for FeCo alloy nanoparticles and  $\gamma$ -Al<sub>2</sub>O<sub>3</sub> matrix by sol-gel approach followed by supercritical drying. The prepared magnetic aerogel was characterized by different techniques. The resultant magnetic aerogel was mesoporous



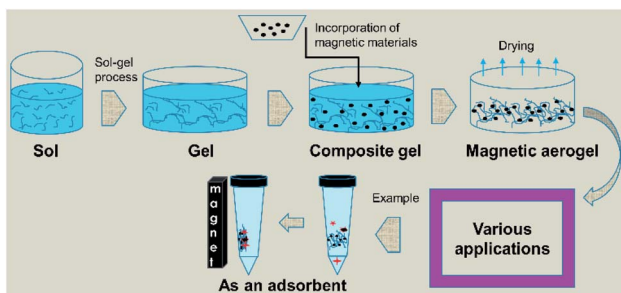


Fig. 6 Generalized representation of a sol-gel process followed by drying for achieving silica-based magnetic aerogel for various applications with an example of adsorption and separation.

had a low density ( $30 \text{ mg cm}^{-3}$ ), the high surface area of  $500 \text{ m}^2 \text{ g}^{-1}$  in untreated form but it got reduced to  $200 \text{ m}^2 \text{ g}^{-1}$  when treated at temperature up to  $900 \text{ }^\circ\text{C}$ .<sup>71</sup> To enhance the catalytic reforming of the  $\text{CH}_4\text{-CO}_2$  aerogel composite made of alumina with cobalt as additive. The composite aerogel greatly improved the efficiency of the fluidized bed reactor under the influence of the axial magnetic field. The catalyst deactivation due to carbon deposition was much lower and the conversion of  $\text{CH}_4$  due to the use of cobalt-based aerogel was several folds higher than that of conventional and fixed bed operations.<sup>72</sup>

It was found that most of the silica-based magnetic aerogels were prepared by following the sol-gel synthesis route followed by the drying process. A simple and generalized schematic representation of fabrication and application of silica-based magnetic aerogel is given as Fig. 6.

### 3. Natural and synthetic polymer-based magnetic aerogels

Magnetic aerogels made of natural/bio and synthetic polymers as a matrix have been successfully utilized for a variety of applications.<sup>73-77</sup> Different strategies were adopted to get the final magnetic aerogel with the desired properties. However, natural and synthetic polymers-based magnetic aerogels were prepared by directly incorporating the magnetic particles into the matrix, the coating on the prepared aerogels, or grown during the synthesis process.

In this section only those natural especially cellulose and other polymeric based aerogels are compiled that involve non-pyrolytic or calcination processes or in other words in which these materials maintain their original structures.

Several types of magnetic cellulose-based aerogels were reported for applications in various advanced applications. The morphological, mechanical, and magnetic properties are usually dependent on the composition and method of fabrication of these materials. These materials are expected to grow more to be able for practical use in the future.<sup>75,78</sup>

Most of the reported natural and synthetic polymers-based magnetic aerogels were mostly used for environmental remediation such as adsorption and degradation of dyes and oils, adsorption of heavy metals along with other studies on biomedical, sensing, electronics, *etc.* as well.

Magnetic nanocellulose based aerogel was prepared by mechanical mixing of nanocellulose, oleic acid, and magnetic nanoparticles and then drying by a freeze-drying process. The resultant aerogel was porous with low density ( $9.2 \text{ mg cm}^{-3}$ ) and exhibited a large surface area ( $397.5 \text{ m}^2 \text{ g}^{-1}$ ) which made it a good adsorbent. Due to the hydrophobic and magnetic nature, it showed an adsorption capacity of  $68.66 \text{ g g}^{-1}$  for cyclohexane and also produced good results for oils and other organic solvents. Therefore, it was thought to be useful in the removal of oil spoilage and other environmental contaminants.<sup>79</sup> Carbonaceous fibers aerogel with the magnetic property was obtained from the pyrolysis of natural cotton containing magnetic iron oxide particles and used for removal of organic solvents and oils and had produced excellent adsorption capacity. Due to the environmentally friendly nature of the carbon source, the high surface area, high superparamagnetic ability ( $M_s 45 \text{ emu g}^{-1}$ ) made this aerogel an excellent adsorbent for oils and organic solvents. It showed a maximum adsorption capacity of 8–10 times of its weight.<sup>80</sup> Cellulose gel containing magnetic particles coated with titanium oxide particles were produced by sol-gel approach and passed through the supercritical drying process to obtain an aerogel with low cost, hydrophobic and paramagnetic ability for efficient removal of contaminants from water sources. The given results showed that the aerogel was able to uptake oils in a quantity equal to 28 times of its weight. The oil adsorption by this cellulosic magnetic aerogel is shown by photographs given in Fig. 7.<sup>81</sup> A simple and a cost-effective hydrothermal method consisting of first making the solutions followed by supercritical drying process was employed for obtaining magnetic nanoparticle-based cellulose aerogel with superparamagnetic property ( $M_s 6.7 \text{ emu g}^{-1}$ ). The magnetic aerogel acted as a catalyst and speeded up the degradation for degradation (97–100%) of Rhodamine B dye by the virtue of Fenton like reaction as shown in Fig. 8.<sup>82</sup>

Cellulose hydrogel incorporated with cobalt ferrite particles was transformed into aerogel by freeze-drying. The resultant aerogel maintained a high surface area ( $270 \text{ m}^2 \text{ g}^{-1}$ ), light-weight ( $250\text{--}390 \text{ mg cm}^{-3}$ ), porosity (78%), and high flexibility.

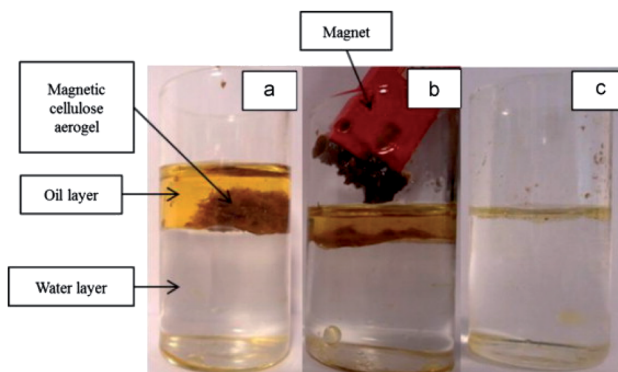


Fig. 7 Photograph of (a) magnetic cellulose/TiO<sub>2</sub> aerogel in oil/water mixture; (b) magnetic cellulose/TiO<sub>2</sub> aerogel can be removed by a magnet and (c) the oil layer on water surface was removed. This figure has been adapted/reproduced from ref. 81 with permission from Elsevier, under the license number 4957790016317, copyright 2020.



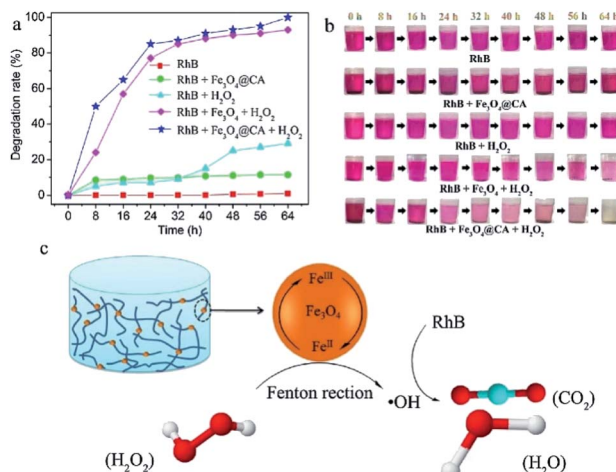


Fig. 8 (a) Degradation kinetics and (b) color changes of RhB solution treated with four kinds of different ingredients, *i.e.*, (I) Fe<sub>3</sub>O<sub>4</sub>@CA, (II) H<sub>2</sub>O<sub>2</sub>, (III) Fe<sub>3</sub>O<sub>4</sub> + H<sub>2</sub>O<sub>2</sub> and (IV) Fe<sub>3</sub>O<sub>4</sub>@CA + H<sub>2</sub>O<sub>2</sub>. (c) Mechanism diagram of RhB degradation by Fenton-like reaction. This figure has been adapted/reproduced from ref. 82 with permission from Elsevier, under the license number 4957790319930, copyright 2020.

Due to the very small size of cobalt ferrite particles, the magnetic ability was very small nearly zero and no hysteresis loop was observed for this aerogel.<sup>83</sup> Manganese ferrite nanoparticles-based carboxylated cellulose aerogel was prepared by *in situ* coprecipitation method followed by surface modification using sodium periodate and sodium chlorite as oxidants. Sol-gel followed by supercritical drying approach was followed to obtain the magnetic aerogel. The obtained magnetic aerogel was having a surface area of 87 m<sup>2</sup> g<sup>-1</sup>. A high adsorption capacity (73.70 mg g<sup>-1</sup>) for Cu(II) was achieved. The adsorbent was easily reusable due to ease in the collection of each use.<sup>84</sup> Cellulose-based aerogel decorated with magnetic iron oxide nanoparticles was prepared by freeze-drying. It was applied for the adsorption of Cr(vi) ions from an aqueous solution. The prepared magnetic aerogel also showed good uptake capacity (22 mg g<sup>-1</sup>) for Cu(II) ions while maintained its high ferromagnetic property (53.69 emu g<sup>-1</sup>).<sup>85</sup> In another effort manganese ferrite containing cellulose-based aerogel was prepared using *in situ* fabrication method by first preparing the hydrogel matrix followed by the supercritical drying process. The obtained aerogel was reported with a high specific surface area (236–288 m<sup>2</sup> g<sup>-1</sup>), porosity, and superparamagnetic property (18.53 emu g<sup>-1</sup>). It showed an uptake capacity of 63.3 mg g<sup>-1</sup> for Cu(II) ions from aqueous solution. Due to having a green synthesis root and biocompatible nature the aerogel was considered suitable for environmental and biological applications.<sup>86</sup> Iron oxide nanoparticles dispersed in a suspension of cellulose extracted from the waste paper was transformed into magnetic aerogel ( $M_s \sim 2.2$  emu g<sup>-1</sup>) by casting and freeze-drying process. The aerogel was successfully used for the adsorption of 1 ppm Congo red dye from an aqueous solution.<sup>87</sup> One step pyrolysis process in the organ atmosphere was used for the fabrication of magnetic aerogel from iron nitrate coated cellulose. The aerogel maintained the paramagnetic behavior



Fig. 9 Schematic illustration of the removal mechanism of Cr(vi) on Fe<sub>3</sub>O<sub>4</sub>@bagasse@chitosan (FBC) aerogel. This figure has been adapted/reproduced from ref. 89 with permission from Elsevier, under the license number 4957791186831, copyright 2020.

and adsorption ability of 29–70 times their weight for oils and organic solvents from the water surface even after ten times the recycling process. It was also found that the aerogel can be made bidirectional adsorbent by thermal treatment.<sup>88</sup> The hydrothermal process followed by the freeze-drying was used to transform waste bagasse fiber and chitosan mixed with magnetic nanoparticles into a composite aerogel with the superparamagnetic property. The as-prepared magnetic aerogels were used for adsorption of Cr(vi) from aqueous solution. The adsorption experiments study showed high adsorption capacity (41 mg g<sup>-1</sup>) for Cr(vi) with easy recovery of the aerogel from the solution. The mechanism of Cr(vi) adsorption is illustrated in Fig. 9.<sup>89</sup>

Magnetic aerogels consisted of bulk cellulose and magnetic particles were prepared by growing magnetic particles on the cellulose chains followed by hot pressing to provide the resultant aerogels with the paramagnetic ability ( $M_s \sim 1$  emu g<sup>-1</sup>) and biodegradability. These aerogels were reported to be suitable for bio-compatible, data storage applications, and other military purposes.<sup>90</sup> Composite magnetic aerogels in the form of monolith and microspheres were synthesized by dispersing maghemite iron nanoparticles in pectin based matrix using the emulsion-gelation method. After the drying process a porous and highly magnetic aerogel was obtained which was considered useful considered for several biomedical applications based on its low density (110 mg cm<sup>-3</sup>), high porosity (~95%) and surface area (284 m<sup>2</sup> g<sup>-1</sup>) while had also shown paramagnetic nature ( $M_s \sim 1$  emu g<sup>-1</sup>). Due to low magnetic behavior, it was recommended for magnetic resonance imaging and targeted drug delivery applications where small magnetic ability is required.<sup>91</sup> Bacterial cellulose nanofibril incorporated with ferromagnetic cobalt ferrite nanoparticles were transformed into highly porous (~99%) magnetic aerogels having low density (15–30 mg cm<sup>-3</sup>), high surface area and flexibility (90% strain) as well as excellent paramagnetic behavior (~300 kA m<sup>-1</sup>). They were suggested for use in designing electronic actuators and microfluidics devices.<sup>91</sup> A simple oxidative coprecipitation synthesis method was used to disperse cobalt ferrite nanoparticles into the cellulose aerogel and obtain a composite magnetic aerogel. The prepared aerogel was highly magnetic (8.6 emu g<sup>-1</sup>) and considered as a potential candidate



for magnetic property sensors and other applications.<sup>92</sup> A facile way of preparing a magnetic aerogel composite was presented by using pure nanocellulose fibers obtained from APMP as a matrix for the dispersion of cobalt ferrite particles and then transformed them into aerogel by sol-gel process. High saturation magnetization value ( $50.024 \text{ emu g}^{-1}$ ) was considered an aid for using it in several potential applications.<sup>93</sup>

Several studies utilizing synthetic polymer alone or in combination with natural polymers are also reported for the fabrication of the magnetic aerogels for various applications. A magnetic composite aerogel consisted of a polyaniline/poly(vinyl alcohol) matrix incorporated with hexaferrite was synthesized for adsorption of Reactive Black 5 dye from an aqueous medium. Due to having a highly elastic nature, superparamagnetic behavior ( $M_s 7.7\text{--}12.5 \text{ emu g}^{-1}$ ), high adsorption ability (99% recovery of reactive black dye from aqueous solution), and possessing electrical conductivity ( $0.32 \text{ S cm}^{-1}$ ), these aerogels were considered a suitable candidate for wastewater treatment and several other potential applications.<sup>77</sup> For decontamination of water from malachite green dye, a 3D magnetic aerogel composite made of bacterial cellulose nanofibers, graphene oxide, and polyvinyl alcohol was prepared by filler loaded approach. This magnetic composite aerogel showed excellent characteristics (surface area  $214.75 \text{ m}^2 \text{ g}^{-1}$ , density  $6.8 \text{ mg cm}^{-3}$  and  $M_s 58.13 \text{ emu g}^{-1}$ ) for the removal of malachite green from real water samples (adsorption capacity  $270.27 \text{ mg g}^{-1}$ ).<sup>94</sup> An aerogel consisted of cellulose and PVA matrix decorated with iron oxide nanoparticles was prepared for adsorption of methyl blue dye ( $27.82 \text{ mg g}^{-1}$ ) and was considered useful for adsorption and degradation of other dyes and pollutants. The obtained aerogel was highly porous, magnetic ( $9.1 \text{ emu g}^{-1}$ ), and mechanical strong.<sup>95</sup> Porous magnetic iron oxide particles interconnected the graphene layers were dispersed in polystyrene-based aerogel. The resultant aerogel with a density of  $\sim 5 \text{ mg g}^{-1}$  was having very high superparamagnetic ability ( $80.8 \text{ emu g}^{-1}$ ). It was used to absorb a high amount of oil ( $\sim 40$  times its weight) from the water surface repeatedly and was able to be squeezed due to high flexibility and good mechanical strength.<sup>73</sup> Magnetic composite aerogel prepared from a gel consisted of cross-linked organosilicon-modified poly(amidoamine) dendrimer, coupled with iron oxide nanoparticles and poly(vinyl alcohol). The prepared magnetic aerogel (surface area  $8 \text{ m}^2 \text{ g}^{-1}$  and  $M_s \sim 30 \text{ emu g}^{-1}$ ) was utilized for oil removal from water surface and showed high adsorption capacity ( $22.9 \text{ g g}^{-1}$ ).<sup>96</sup> Different amounts of magnetic nanoparticles were dispersed within the iota-carrageenan and polyamidoamine dendrimer matrix during their physical crosslinking. The resultant magnetic aerogel with a high surface area ( $385 \text{ m}^2 \text{ g}^{-1}$ ) produced good results for Cr(vi), Cu<sup>2+</sup>, Cd<sup>2+</sup>, Mn<sup>7+</sup>, Co<sup>2+</sup>, and Alphanol fast blue dye. Among the heavy metal ions, the maximum adsorption capacity was observed for Cu(II) with a recovery of 99% whereas 97% of Alphanol fast blue dye was also recovered.<sup>97</sup> Magnetic propylene oxide-based aerogel was synthesized by a sol-gel approach followed by supercritical drying. The obtained aerogel was having low density ( $249\text{--}393 \text{ mg cm}^{-3}$ ) and superparamagnetic ( $14.64\text{--}52.28 \text{ emu g}^{-1}$ ) nature. It was also deduced from the study that

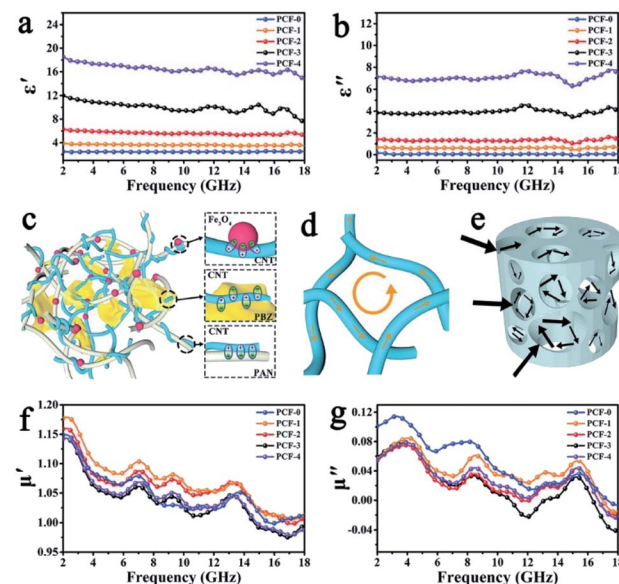


Fig. 10 Frequency dependence of (a) real part  $\epsilon'$  and (b) imaginary part  $\epsilon''$  of complex permittivity. Scheme of (c) interfacial polarization, (d) microcurrent loss, and (e) multiscattering in aerogel. Frequency dependence of (f) real part  $\mu'$  and (g) imaginary part  $\mu''$  of complex permeability. This figure has been adapted/reproduced from ref. 99 with permission from John Wiley and Sons, under the license number 4957800340877, copyright 2020.

the concentration and drying conditions play a vital role in controlling the final texture, structural, and magnetic properties of the aerogel. The produced aerogel was considered suitable for microwave absorption applications.<sup>98</sup> An ultralight and ultrathin 3D aerogel with the main skeleton made from polybenzoxazine cross-linked polyacrylonitrile fibers with carbon nanotubes and magnetic iron oxide particles as dispersed additive was prepared by simple dispersion followed by freeze-drying and low temperature ( $235 \text{ }^\circ\text{C}$ ) heat treatment in inert atmosphere for 2 h. Multicomponent magnetic aerogel was studied for its microwave absorption property which produced excellent absorption results due to the combined effect of multicomponents of the organic and inorganic origin of the aerogel as shown in Fig. 10.<sup>99</sup>

#### 4. Carbon-based magnetic aerogels

Like silica aerogels, the carbon-based aerogels are one of the most studied aerogels with a basic focus on their application as a catalyst for dyes degradation and oil removal from water bodies, microwave absorption, electromagnetic interference and electroanalytical applications.<sup>100-103</sup>

Magnetic carbon aerogels mostly involve calcination process which may or may not be followed by surface modification. In order to maintain the superparamagnetic behavior of the aerogel, the calcination temperature is maintained within the optimum range. However, from the present review we also found that in some cases the pyrolysis or calcination is not performed and the carbon-based materials such as graphene,



graphene oxide, carbon nanotubes *etc.* are utilized in combination with other materials to obtain the magnetic aerogels.

Although cellulose and other natural and synthetic polymeric-based aerogels are already covered in the previous section but in here we will focus on carbon aerogels that are prepared by pyrolysis or calcination of these materials. Some more types not involving these materials are also discussed.

A bio-based carbon aerogel was prepared by the carbonization of popcorn as the raw material. For this purpose, the raw material was dipped in magnetic particles solution followed by drying at 60 °C and then carbonization to obtain the magnetic carbon aerogel. The aerogel was surface modified to make it hydrophobic. The synthesized magnetic aerogel had a low density (950 mg cm<sup>-3</sup>), high surface area (229.25 m<sup>2</sup> g<sup>-1</sup>), and suitable magnetic property (3.3 emu g<sup>-1</sup>) that showed an adsorption capacity value of 10.2 g g<sup>-1</sup> for oils and organic solvents from the water surface.<sup>104</sup> Cotton balls were decorated with magnetic nanoparticles were carbonized to obtain a magnetic carbon aerogel with very low density (~2 mg cm<sup>-3</sup>) and porosity (~99.9%) for oil separation from the water surface. Due to having superhydrophobicity and super oleophilicity the reported aerogel showed an uptake capacity of 61–113 g g<sup>-1</sup> and was also considered suitable for removal of other nonpolar pollutants and energy storage applications.<sup>105</sup> A conducting and magnetic aerogel consisting of a double network of graphene and decorated with magnetic iron oxide particles was produced by supercritical drying of the hydrogel material followed by the carbonization process. The schematic illustration of the synthesis process is given in Fig. 11. The density (30–65 mg cm<sup>-3</sup>), surface area (270–414 m<sup>2</sup> g<sup>-1</sup>), saturation magnetization (23–54 emu g<sup>-1</sup>) and electrical conductivity (0.5–5 × 10<sup>-2</sup> S cm<sup>-1</sup>) were all suitable acquiring multiple applications. However, the obtained aerogel was immobilized with  $\beta$ -

glucuronidase (loading capacity 2.45 mg g<sup>-1</sup>) for the biocatalytic transformation (98%) of glycyrrhizin into its product components.<sup>106</sup>

Ferric trichloride, collagen, and carboxymethyl cellulose were used as precursors to fabricate magnetic nitrogen-doped carbon aerogel. A simple sol–gel approach was used to prepare a sol of the precursors followed by freeze-drying and carbonization processes. The prepared magnetic aerogels were activated with KOH solution and were used as electrode materials due to their conducting nature (capacitance 156.9 F g<sup>-1</sup>) and as an adsorbent for adsorption of malachite green and methylene blue dye. The adsorption capacities of 238.2 and 230.4 mg g<sup>-1</sup>, respectively were achieved for these two dyes. From the obtained results it was concluded that this aerogel has the potential to be used in making supercapacitors and adsorbents for environmental remediation.<sup>107</sup> Magnetic carbon aerogel made from konjac glucomannan with magnetic iron and manganese oxides as additive was synthesized by sol–gel followed by carbonization process at 500 °C in an inert atmosphere and were used for the adsorption of anionic and cationic dyes from aqueous solutions. The surface area of the resultant aerogel was 32.11 m<sup>2</sup> g<sup>-1</sup> while it maintained a high superparamagnetic nature with saturation magnetization value of 64.87 emu g<sup>-1</sup> which were able to successfully recover methyl orange (9.37 mg g<sup>-1</sup>) and methyl blue (10.93 mg g<sup>-1</sup>) from the aqueous media.<sup>108</sup> Ultralight (~1 mg cm<sup>-3</sup>) and a superparamagnetic ( $M_s \sim 7.1$  emu g<sup>-1</sup>) carbon aerogel was prepared from tubular cellulose incorporated with magnetic particles by a multistep process of solution, freeze drying and pyrolysis. The aerogel showed high compressibility, electrical conductivity, fire ret ardency, and high adsorption capacity (147–292 g g<sup>-1</sup>) for organic pollutants.<sup>109</sup> Carbon aerogel incorporated with iron oxide nanoparticles was synthesized by sol–gel, freeze drying and pyrolysis in an inert atmosphere and then mixed with an ionic liquid to produce a composite aerogel film for use as a biocompatible interface and bioelectrocatalyst for speeding up the electrochemistry glucose oxidase and myoglobin as well as reduction hydrogen peroxide reduction respectively. Furthermore, this aerogel had a high surface area (676 m<sup>2</sup> g<sup>-1</sup>) and showed a broad linear response to hydrogen peroxide which makes it a better candidate for future application as biosensors.<sup>110</sup> A nickel/carbon aerogel (density 120 mg cm<sup>-3</sup>, surface area 522 m<sup>2</sup> g<sup>-1</sup>) with conductive nature and the controllable magnetic property ( $M_s$  4.7 emu g<sup>-1</sup>) was synthesized by first making a hydrogel followed by supercritical drying and finally the pyrolysis process at 1050 °C in an inert atmosphere. In addition to electrical conductivity (0.1 S cm<sup>-1</sup>) and super-paramagnetic behavior ( $M_s$  4.7 emu g<sup>-1</sup>), the resultant aerogels were nanoporous in structure with the high specific surface area. These all properties made it an efficient microwave absorbing material with excellent performance (RL –57 dB at 13.3 GHz).<sup>28</sup> Magnetic aerogel with different additives including magnetic iron oxide, cobalt, and nickel foam was synthesized by mixing the pre-synthesized modified polyurethane sponges and the precursors of above additives, followed by the heat treatment in inert atmosphere. The carbon matrix of the aerogel was obtained by calcination of polyurethane grafted with

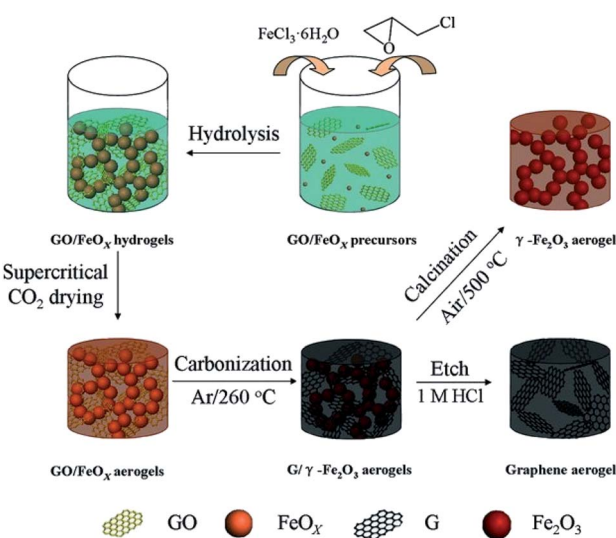


Fig. 11 Illustration of the synthetic route for single-network of the graphene and  $\text{Fe}_2\text{O}_3$  aerogels and double-network of the hybrid graphene/ $\text{Fe}_2\text{O}_3$  aerogels. This figure has been adapted/reproduced from ref. 106 with permission from John Wiley and Sons, under the license number 4957800596807, copyright 2020.



polyelectrolyte layers and metal acrylate. The prepared aerogel was super hydrophobic and super oleophilic in nature and showed excellent results for oils and organic solvents ( $\sim 99.9\%$  removal) from the water surface. This aerogel was considered a potential candidate for several important application areas due to its magnetic and physical characteristics (density  $\sim 5\text{ mg cm}^{-3}$  and surface area  $89.5\text{ m}^2\text{ g}^{-1}$ ).<sup>111</sup> Magnetic carbon aerogel was prepared by sol-gel, freeze-drying, and carbonization of iron cross-linked sodium carboxymethyl cellulose. The resultant magnetic carbon aerogel with a saturation magnetization of  $19.97\text{ emu g}^{-1}$  was having low density ( $620\text{ mg cm}^{-3}$ ), high surface area ( $742.34\text{ m}^2\text{ g}^{-1}$ ), flame retardant, hydrophobic aerogel which was considered very useful as a potential adsorbent, magnetic sensor, and catalyst.<sup>112</sup> Sugarcane bagasse-based cellulose doped with N/S was used as a precursor for preparing magnetic carbon aerogel with a high surface area ( $668.3\text{ m}^2\text{ g}^{-1}$ ) and superparamagnetism ( $M_s 40.76\text{ emu g}^{-1}$ ). The synthesis was achieved by freeze-drying the solution mixture of treated bagasse cellulose followed by freeze-drying and carbonization process at  $800\text{ }^\circ\text{C}$  in the presence of argon. It acted as an efficient adsorbent for the removal of bisphenol-A dye (adsorption capacity  $197.6\text{ mg g}^{-1}$ ) from water.<sup>113</sup> Trifunctional iron oxide nanoparticle-based carbon aerogel with a high surface area ( $551\text{ m}^2\text{ g}^{-1}$ ) was prepared for the photocatalytic degradation of Rhodamine B dye present in aqueous samples. The magnetic aerogel was able to be recollected with the help of an external magnet after degrading Rhodamine B in the presence of visible light.<sup>114</sup>

The pristine, partially reduced graphene oxide-based aerogel with small traces of iron and manganese inside its structural network was reported for potential applications in various fields requiring low magnetic materials. The obtained magnetic carbon aerogel was having low density ( $6\text{ mg cm}^{-3}$ ) and weak paramagnetic behavior.<sup>115</sup> Graphene oxide-based magnetic aerogel was fabricated by simply autoclaving the solution of the precursors' solution. The high surface area ( $383.6\text{ m}^2\text{ g}^{-1}$ ) and magnetic property ( $M_s 39.77$ ) of this magnetic carbon aerogel make it an excellent adsorbent for water purification it was suggested for the purification of water from various contaminants such as organic solvents, dyes, and arsenic. It showed a maximum adsorption capacity of  $22$  and  $11.3\text{ mg g}^{-1}$  for gasoline and arsenic, respectively.<sup>116</sup> An aerogel made of N-doped graphene and magnetic iron oxide was fabricated by a multiple-step process consisted of hydrothermal, freeze-drying and heat treatment steps. It was applied as a catalyst for the oxygen reduction reaction. The given results showed that it was found it was having a surface area of  $110\text{ m}^2\text{ g}^{-1}$  and showed better results as a catalyst than the available Pt/C catalyst for the same purpose.<sup>117</sup> The dispersion containing the graphene oxide and magnetite nanoparticles was transformed into highly porous magnetic aerogel powder by hydrothermal treatment and freeze-drying process. Due to the high porosity and the functional surface of the aerogel powder, it showed an excellent adsorption capacity ( $130\text{ mg g}^{-1}$ ) for methylene blue dyes. The resultant aerogel was superparamagnetic ( $2.2\text{ emu g}^{-1}$ ) and was able to be collected by an external magnet.<sup>118</sup> A nanocomposite aerogel composed of iron

oxide and graphene was fabricated by mixing various amounts of iron oxide and graphene oxide while ethylene diamine was used as a reducing agent. The magnetic graphene aerogel was prepared by a sol-gel approach followed by freeze-drying and annealing. The prepared magnetic aerogel ( $M_s 3.4\text{ emu g}^{-1}$ , density  $42\text{ mg cm}^{-3}$ , and surface area  $95.22\text{ m}^2\text{ g}^{-1}$ ) was successfully used as an adsorbent with a maximum adsorption capacity ( $253.80\text{ mg g}^{-1}$ ) for bisphenol-A removal from water. It was also suggested as a suitable material for anode for lithium-ion batteries.<sup>119</sup> The 3D architecture of magnetic, porous, and lightweight graphene/iron oxide aerogel was produced by dispersing iron oxide nanoparticles in graphene oxide and transforming them into aerogel by reduction and drying process. The aerogel was considered applicable for various electronic and other important applications.<sup>120</sup> 3D metal-organic framework and graphene oxide-based aerogel (density  $\sim 14\text{ mg cm}^{-3}$  and surface area  $168\text{ m}^2\text{ g}^{-1}$ ) were produced by self-assembly approach followed by sol-gel process and freeze-drying. The aerogels showed excellent photocatalytic activity for the degradation of various pollutants present in water.<sup>121</sup>

A magnetic aerogel composed of mesoporous iron oxide and cross-linked carbon nanotubes was synthesized by using the *in situ* growth method involved for the sol-gel process followed by autoclave treatment and freeze-drying. This magnetic aerogel made of iron oxide nanoparticles threaded by carbon nanotubes was of low density ( $12\text{ mg cm}^{-3}$ ), high surface area ( $125\text{ m}^2\text{ g}^{-1}$ ) and possessed mesoporosity was used for microwave absorption ( $RL - 25\text{ dB}$ ) and was considered suitable for other potential applications also.<sup>122</sup> A special technique of aerogel-sol-hydrogel with drying by freeze-drying or supercritical drying methods for the synthesis of magnetic carbon nanotubes based aerogels were applied. The aerogels presented low density ( $12 - 14\text{ mg cm}^{-3}$ ), high surface area ( $182 - 196\text{ m}^2\text{ g}^{-1}$ ), superparamagnetic magnetic property, and a good adsorption capacity for methylene blue ( $103\text{ mg g}^{-1}$ ).<sup>123</sup>

Superparamagnetic nickel and graphene nanosheets were mixed and transformed into magnetic composite aerogel by hydrothermal reduction and pyrolysis processes in such a way that the first solution of the components was prepared which was followed by freeze-drying and then calcinations process at  $550\text{ }^\circ\text{C}$  for  $3\text{ h}$  in an argon atmosphere. Due to the lightweight ( $20\text{ mg cm}^{-3}$ ), high surface area ( $544\text{ m}^2\text{ g}^{-1}$ ), wider absorption frequency range, conductive and magnetic nature of the aerogel it was used for microwave absorption purposes ( $RL_{min} - 5.38\text{ dB}$ ). A schematic illustration for microwave absorption by this aerogel is depicted as Fig. 12.<sup>42</sup>

CoNi and reduced graphene oxide-based aerogel with very low density and thickness was produced by similar *in situ* solvothermal and carbonization process as described above. However, here the pyrolysis was performed at  $900\text{ }^\circ\text{C}$  for  $2\text{ h}$  in an argon atmosphere. The prepared magnetic carbon aerogel was used for microwave absorption applications which produced good results ( $RL_{min} - 53\text{ dB}$ ). According to the authors, the highly porous structure, large surface area and the distribution of Co/Ni nanospheres onto the surface of the reduced graphene oxide aerogel matrix made it a suitable



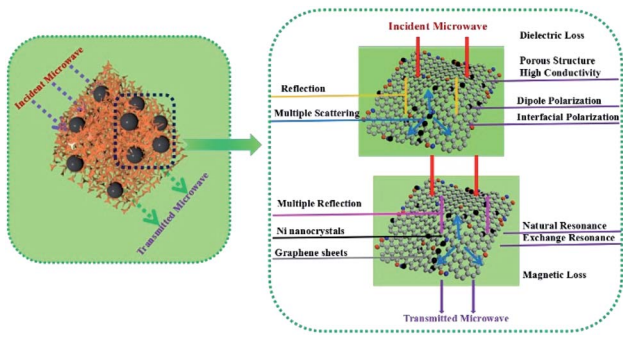


Fig. 12 Schematic illustration of MA mechanism of GA@Ni composites. This figure has been adapted/reproduced from ref. 42 with permission from Elsevier, under the license number 4957801367456, copyright 2020.

candidate for microwave absorption and storage applications.<sup>124</sup>

The  $\text{Fe}_3\text{O}_4$ /phenol-formaldehyde resin was used as a precursor for the production of iron/carbon aerogel by using the similar process described in the previous two cases with the only difference of using 400 and 800 °C for 6 h in a nitrogen atmosphere. The surface area and saturation magnetization was also calculated as  $487 \text{ m}^2 \text{ g}^{-1}$  and  $40.9 \text{ emu g}^{-1}$ , respectively. The purpose of this aerogel was to use it as an adsorbent for arsenic ions removal from water. The aerogel adsorbent showed excellent adsorption capacity ( $216.9 \text{ mg g}^{-1}$ ) towards As(v) and maintained high paramagnetic behavior which made it easy for recollection and reuse.<sup>125</sup> Polymeric and colloidal carbon aerogels were produced by first preparing resorcinol-formaldehyde aerogel by sol-gel and freeze-drying and then converting it into carbon aerogel pyrolysis. The final aerogel was then studied for transport and magnetic properties on the basis of their morphological characteristics (density  $117 \text{ mg cm}^{-3}$ , and surface area  $800 \text{ m}^2 \text{ g}^{-1}$ ). It was found that the electrical and magnetic properties of the aerogel were dependent on the grain size and the mass density of the prepared carbon aerogel.<sup>126</sup> Iron carbide and carbon-based magnetic aerogel was obtained by the citrate sol-gel and annealing process at 800 °C for 1 h in a nitrogen atmosphere. The resultant aerogel exhibited a mesoporous structure with the high specific surface area ( $290 \text{ m}^2 \text{ g}^{-1}$ ) which produced excellent results (adsorption capacity  $56.2 \text{ mg g}^{-1}$ ) as an adsorbent for removal of As(v) from aqueous solution.<sup>41</sup>

## 5. Miscellaneous magnetic aerogels

Although the magnetic aerogels made of only metals or metal oxides and clay with magnetic materials are not broadly explored but the reported studies give an indication of their potential applications in several areas. Much more research is needed in these types of magnetic aerogels to explore their worth, however, from the brief overview of the reported studies much can be extracted in terms of their importance. These are fabricated directly by transforming the magnetic particles alone or mixed with some other metals and metal oxide particles into

aerogels. These aerogels offer high degree of electrical, catalytic, and magnetic characteristics which are suitable for catalytic degradation, purification, sensing, biomedical and electronics applications.

Magnetic aerogel composed of only iron oxide was prepared by converting the iron oxide solution into amorphous aerogel by heating them in the inert atmosphere of argon. To convert the resultant amorphous aerogel to crystalline form it was further treated at high temperature in the presence of air. The resultant magnetic aerogel was having maximum saturation magnetization value of  $9.1 \text{ emu g}^{-1}$ . It was concluded from their study that the magnetic property of the prepared iron oxide aerogel was dependent on the temperature such as at a high temperature it acted as superparamagnetic but at low temperature, its magnetic ability decreased due to magnetic interaction.<sup>127</sup> Transparent conductive oxide films are very useful for obtaining several important optical, electronic, and industrial applications. Iron oxide nanoparticles-based aerogel was prepared by following the sol-gel approach to obtain a hydrogel followed by autoclave and heat treatment in an oven at 500 °C in the presence of air. It had a magnetic and conducting nature (in the case of aluminum-doped was the highest). It was also concluded from this study that the final structural and magnetic properties of the transparent conductive oxide films can be controlled by means of changing the synthetic protocols.<sup>128</sup> The iron and cobalt alloy based particles were prepared within the alumina aerogel by multiple steps process of first preparing a hydrogel followed by autoclaving and two steps calcination at high temperature in the presence of air and then in inert atmosphere or simply reduced in the presence of hydrogen using high temperature. The size and amount of the particles produced depend on the temperature and reduction time during the calcination process. The prepared composite aerogels showed low density ( $30 \text{ mg cm}^{-3}$ ), high surface area ( $564.22 \text{ m}^2 \text{ g}^{-1}$ ) superparamagnetic behavior which was considered to be dependent on the particle size of the distributed iron-cobalt alloy particles within the aerogel matrix.<sup>129</sup> Zinc ferrite aerogels were produced by sol-gel and drying approach and then post-treated in two different ways to check the magnetic behavior of the resultant aerogel particles. The calcinated aerogel powder showed lower magnetic property while the ball-milled aerogel powder magnetic properties were retained with an increase in the inversion parameter. A high maximum saturation magnetization value was reported as  $73 \text{ emu g}^{-1}$  which showed its very high superparamagnetic nature.<sup>130</sup> Magnesium ferrite and magnesium chromite-based aerogels were prepared by drying their prepared hydrogel using the supercritical drying process. The morphology and structural characteristics of the two types of aerogels were noticed to be different from each other. The surface area of magnesium ferrite aerogel was  $131 \text{ m}^2 \text{ g}^{-1}$  while that of magnesium chromite aerogel was  $198 \text{ m}^2 \text{ g}^{-1}$ . Magnesium ferrite based aerogel showed n-type semiconductor behavior and the magnesium chromite based showed p-type.<sup>131</sup> In order to fabricate a magnetic aerogel for photocatalytic degradation Rhodamine B dye core-shell  $\text{Fe}_3\text{O}_4@\text{TiO}_2$  particles were dispersed in silica aerogel by using the sol-gel approach and hydrothermal drying process. The obtained composite





Table 1 Summarized representation of different potential applications of various types of magnetic aerogels

| Magnetic aerogels       |   |
|-------------------------|---|
| Types                   | Silica/alumina based  |
| Properties <sup>a</sup> | Density: ~30 to 620 (mg cm <sup>-3</sup> )<br>Porosity: ~62 to >90%<br>Surface area: ~86–957 (m <sup>2</sup> g <sup>-1</sup> )<br>Magnetic value: ~0.1 to 198 (emu g <sup>-1</sup> )<br>Hyperthermia therapy application <sup>48</sup><br>Radiotherapy and diagnostic applications <sup>64</sup><br>Magneto-optic sensors and magnetic devices <sup>44</sup>  |
| Therapeutic/ Diagnostic | Cellulose/polymers based<br>Density: ~9 to 390 (mg cm <sup>-3</sup> )<br>Porosity: ~78 to 99%<br>Surface area: ~8 to 397 (m <sup>2</sup> g <sup>-1</sup> )<br>Magnetic value: ~1 to 81 (emu g <sup>-1</sup> )<br>Potential biological applications <sup>86</sup><br>Sensor and other applications <sup>92</sup>   |
| Water purification      | Metal oxide/clay based<br>Density: ~4 to 681 (mg cm <sup>-3</sup> )<br>Porosity: highly porous<br>Surface area: ~95 to 564 (m <sup>2</sup> g <sup>-1</sup> )<br>Magnetic value: ~3 to 65 (emu g <sup>-1</sup> )<br>Potential application as biosensors <sup>110</sup>   |
|                         | Adsorption/degradation of methylene blue dyes, <sup>118</sup> Rhodamine B in the presence of visible light, <sup>114</sup> Malachite green and <sup>107</sup> Methylene blue dyes, <sup>107</sup> Bisphenol-A dye, <sup>113</sup> dyes, <sup>108</sup> Bisphenol A <sup>119</sup><br>Oils and organic solvents removal from water surface <sup>104,135</sup>  |
|                         | Adsorption of Rhodamine B from aqueous solution <sup>45</sup><br>Adsorption of As(m) at optimized conditions <sup>336</sup>   |
|                         | Oil spoilage and other environmental contaminants removal <sup>73,79,81,88,95,96</sup><br>Organic pollutants <sup>109</sup><br>Adsorption of multiple cations and oxyanions <sup>97</sup><br>Adsorption of Pb <sup>2+</sup> and Cu <sup>2+</sup> ions, <sup>85</sup> Cr <sup>VI</sup> <sup>89</sup><br>Immobilization of catalase <sup>138</sup><br>Microwave absorption property <sup>98,99</sup><br>Data storage applications and other military purposes <sup>00</sup> |
| Enzyme immobilization   | Immobilization of <i>Candida rugosa</i> lipase enzyme <sup>49</sup><br>Microwave absorption property <sup>139</sup>   |
| Defense                 | Use in designing electronic actuators and microfluidics devices <sup>31</sup>   |
| Miscellaneous           | Conversion of CO to methane gas <sup>24</sup><br>Capture of hypervelocity microparticles catalytic reforming of the CH <sub>4</sub> –CO <sub>2</sub> (ref. 72)  |
|                         | —   |
|                         | Carbon based<br>Density: ~1 to 950 (mg cm <sup>-3</sup> )<br>Porosity: ~99%<br>Surface area: ~90 to 742 (m <sup>2</sup> g <sup>-1</sup> )<br>Magnetic value: ~3 to 65 (emu g <sup>-1</sup> )<br>Potential application as biosensors <sup>110</sup>  |
|                         | Adsorption/degradation of methylene blue dyes, <sup>118</sup> Rhodamine B in the presence of visible light, <sup>114</sup> Malachite green and <sup>107</sup> Methylene blue dyes, <sup>107</sup> Bisphenol-A dye, <sup>113</sup> dyes, <sup>108</sup> Bisphenol A <sup>119</sup><br>Oils and organic solvents removal from water surface <sup>104,135</sup>  |
|                         | Adsorption of As(v) <sup>41,114</sup>   |
|                         | —   |
|                         | Microwave absorbing material <sup>28,42,122,124,140,141</sup>   |
|                         | —   |
|                         | Energy storage application <sup>105</sup>   |
|                         | Potential magnetic sensor, electronics, and catalysts <sup>52,112,117,120,121</sup>   |

<sup>a</sup> Based on the data mentioned in the references cited in this paper.

aerogel was superparamagnetic in nature ( $M_s$  60–90 emu g<sup>-1</sup>). It was used in catalytic degradation of Rhodamine B from an aqueous solution and showed good results (94%).<sup>45</sup> Lanthanum based aerogels were synthesized by the sol-gel process followed by supercritical fluid drying. From this study, it was found that if the prepared aerogels are treated at 600 °C in the air they are converted to porous nanostructures of La(OH)<sub>3</sub> having magnetic properties suitable for various potential applications.<sup>22</sup> Solvothermal and hydrothermal processes preceded by drying in the vacuum oven at 55 °C for 24 h were applied to obtain the multiple components magnetic composite aerogel consisting of reduced graphene doped with nitrogen, and nickel oxide as well as zinc oxide ferrite (NRGO/Ni0.5Zn0.5Fe<sub>2</sub>O<sub>4</sub>). The obtained aerogel was highly magnetic ( $M_s$  64.8 emu g<sup>-1</sup>) and produced excellent results for microwave absorption application ( $RL_{min}$  –63.2 dB).<sup>132</sup> Manganese iron oxide-based hydrogels were prepared from their chlorides precursors by the sol-gel method followed by supercritical CO<sub>2</sub> extraction. The prepared aerogel was reported with high surface area (489 m<sup>2</sup> g<sup>-1</sup>) and possessed superparamagnetic magnetic behavior ( $M_s$  ~40 emu g<sup>-1</sup>).<sup>133</sup> Ultralight (8–10 mg cm<sup>-3</sup>), magnetic nanofibrous GdPO<sub>4</sub> aerogel (with a surface area 29–35 m<sup>2</sup> g<sup>-1</sup>) was prepared by the hydrothermal method followed by freeze-drying and calcination processes. Interestingly, in this study, no other magnetic additive and matrix material was used and the resultant aerogel was highly magnetic in nature due to the magnetic nature because of the strong paramagnetic nature of Gd<sup>3+</sup> ions. This magnetic aerogel was recommended for several potential applications.<sup>134</sup>

A magnetic aerogel with the magnetic property was prepared using sodium carboxymethyl cellulose incorporated with montmorillonite clay by a sol-gel approach followed by freeze-drying and carbonization at high temperature (950 °C in an inert atmosphere). The aerogel had low density (64 mg cm<sup>-3</sup>), high surface area (185 m<sup>2</sup> g<sup>-1</sup>) was highly ferromagnetic (31.10 emu g<sup>-1</sup>) at room, and showed high adsorption capacity (10–20 times its weight) for oils and organic solvents.<sup>135</sup> In order to prepare a clay-based magnetic aerogel adsorbent for As(III) removal, surface modified magnetic iron and manganese oxides were incorporated into Na<sup>+</sup>-MMT reinforced KGM and transformed into an aerogel sol-gel and freeze-drying method. The prepared composite aerogel was having a density in the range of 514–681 mg cm<sup>-3</sup>, highly porous, mechanically stable, and high saturation magnetization value (7–46 emu g<sup>-1</sup>). It showed good adsorption (adsorption capacity 13.30 mg g<sup>-1</sup>) of As(III) at optimized conditions.<sup>136</sup>

## 6. Future perspectives

The unique air-filled highly porous solid network structures and superiority due to their non-toxic, non-flammable, and easily disposable nature compared to most available materials, the aerogels have the potential for high scale and broad range of applications. Modification of the pristine aerogels to obtain the magnetic aerogels have certainly brought innovation in terms of having superparamagnetic nature and enhanced performance. The use of magnetic aerogels for environmental, biomedical, electronic, EMI shielding, microwave absorption, thermal

insulation, data storage, *etc.* are the indications of the future uses of this versatile and futuristic material with extraordinary properties. These are the most demanding tasks to obtain from magnetic aerogels on large scale in the future. Some of the selected studies that reported their potential role in the mentioned areas are summarized in Table 1.

## 7. Conclusion

Aerogels and aerogel composites are known for several important applications. Inducing magnetic property into the aerogels in any way makes them entirely new materials of high significance. Magnetic aerogels serve well than ordinary aerogels owing to possessing magnetic property, due to which they are easily recoverable and reusable, suitable for making excellent electromagnetic and sound proofing coatings, acoustic and electronic materials. Magnetic aerogels are excellent adsorbents and potential candidates for diagnostic, therapeutic, immobilization, defense, *etc.* applications. These are prepared by the different procedures from different types of materials whereas each type has its own consideration regarding cost and final use. We found that silica, polymers, and carbon-based aerogels are the most reported types of matrix materials for the fabrication of magnetic aerogels. However, some studies using alumina, clays, graphene, CNTs, and only magnetic metals-based materials are also conducted. Different types of preparation methods are based on variation in the incorporation methods of magnetic particles inside the matrix and on the drying procedures to get the final product. The magnetic property varies with variation in types of magnetic particles, their concentration, and their incorporation way into the matrix. Magnetic aerogels with higher values of saturation magnetization are mostly recommended for adsorption, catalysis, EMI shielding, electronics, *etc.* whereas those with low saturation magnetization are also recommended for those biomedical/diagnostic applications where small magnetization is required. The production of magnetic aerogels on a large industrial scale is limited probably due to their fabrication cost and handling but owing to their versatile applications, there is a big demand for research in the field of these future-oriented advanced materials. Research is in progress to make these materials available for use on an industrial scale for large-scale applications.

## Funding

This work was done under the 2019–20 Fulbright Visiting Scholar Program funded by the U.S. Department of State. This work is also supported by the National Science Foundation under Award No. 1943445, National Science Foundation under Award No. OIA-1656006 and matching support from the state of Kansas through Kansas Board of Regents, NASA EPSCoR CAN Grant No. 80NSSC19M0153, and Johnson Cancer Centre.

## Conflicts of interest

There are no conflicts to declare.

## Acknowledgements

The first author is indebted to the support of the Institute of International Education; the United States of America and the United States Education Foundation; Pakistan for their cooperation, support, and guidelines during the Fulbright program.

## References

- 1 S. S. Kistler, Coherent Expanded Aerogels and Jellies, *Nature*, 1931, **127**(3211), 741.
- 2 G. Pajonk, A short history of the preparation of aerogels and carbogels, in *Sol-Gel Processing and Applications*, Springer, 1994, pp. 201–219.
- 3 M. Cantin, *et al.*, Silica aerogels used as Cherenkov radiators, *Nucl. Instrum. Methods*, 1974, **118**(1), 177–182.
- 4 J. Fricke and T. Tillotson, Aerogels: production, characterization, and applications, *Thin Solid Films*, 1997, **297**(1–2), 212–223.
- 5 N. Hüsing and U. Schubert, Aerogels—airy materials: chemistry, structure, and properties, *Angew. Chem., Int. Ed.*, 1998, **37**(1–2), 22–45.
- 6 A. C. Pierre and G. M. Pajonk, Chemistry of aerogels and their applications, *Chem. Rev.*, 2002, **102**(11), 4243–4266.
- 7 Y. Wang, *et al.*, The advances of polysaccharide-based aerogels: Preparation and potential application, *Carbohydr. Polym.*, 2019, **226**, 115242.
- 8 R. Du, *et al.*, Emerging noble metal aerogels: state of the art and a look forward, *Matter*, 2019, **1**(1), 39–56.
- 9 C. M. Almeida, M. E. Ghica and L. R. Durães, An overview on alumina-silica-based aerogels, *Adv. Colloid Interface Sci.*, 2020, 102189.
- 10 R. R. Raju, *et al.*, Ultralight magnetic aerogels from Janus emulsions, *RSC Adv.*, 2020, **10**(13), 7492–7499.
- 11 S. G. Mosanenzadeh, *et al.*, Polyimide aerogels with novel bimodal micro and nano porous structure assembly for airborne nano filtering applications, *RSC Adv.*, 2020, **10**(39), 22909–22920.
- 12 P. Suktha, *et al.*, In situ mass change and gas analysis of 3D manganese oxide/graphene aerogel for supercapacitors, *RSC Adv.*, 2019, **9**(49), 28569–28575.
- 13 G. Horvat, *et al.*, Preparation and characterization of polysaccharide-silica hybrid aerogels, *Sci. Rep.*, 2019, **9**(1), 1–10.
- 14 A. Leroy, *et al.*, High-performance subambient radiative cooling enabled by optically selective and thermally insulating polyethylene aerogel, *Sci. Adv.*, 2019, **5**(10), eaat9480.
- 15 O. V. Kharissova, H. R. Dias and B. I. Kharisov, Magnetic adsorbents based on micro-and nano-structured materials, *RSC Adv.*, 2015, **5**(9), 6695–6719.
- 16 M. F. Casula, A. Corrias and G. Paschina, Iron oxide–silica aerogel and xerogel nanocomposite materials, *J. Non-Cryst. Solids*, 2001, **293**, 25–31.
- 17 A. Casu, *et al.*, Magnetic and Structural Investigation of Highly Porous  $\text{CoFe}_2\text{O}_4\text{--SiO}_2$  Nanocomposite Aerogels, *J. Phys. Chem. C*, 2007, **111**(2), 916–922.
- 18 E. Taboada, *et al.*, Faraday rotation measurements in maghemite-silica aerogels, *J. Magn. Magn. Mater.*, 2006, **301**(1), 175–180.
- 19 R. Sui and P. Charpentier, Synthesis of metal oxide nanostructures by direct sol–gel chemistry in supercritical fluids, *Chem. Rev.*, 2012, **112**(6), 3057–3082.
- 20 F. J. Heilitag, *et al.*, Anisotropically structured magnetic aerogel monoliths, *Nanoscale*, 2014, **6**(21), 13213–13221.
- 21 D. Lovskaya and N. Menshutina, Alginate-Based Aerogel Particles as Drug Delivery Systems: Investigation of the Supercritical Adsorption and In Vitro Evaluations, *Materials*, 2020, **13**(2), 329.
- 22 Z. Zhang, *et al.*, Evolution of high specific surface area lanthanum aerogels to magnetic lanthanum hydroxide nanostructures, *Inorg. Chem. Commun.*, 2020, **114**, 107818.
- 23 G. C. Hadjipanayis, *Magnetic storage systems beyond 2000*, vol. 41, 2012, Springer Science & Business Media.
- 24 J. Li, *et al.*, Enhanced methanation over aerogel  $\text{NiCo/Al}_2\text{O}_3$  catalyst in a magnetic fluidized bed, *Ind. Eng. Chem. Res.*, 2013, **52**(20), 6647–6654.
- 25 S.-J. Wang, *et al.*, Floatable magnetic aerogel based on alkaline residue used for the convenient removal of heavy metals from wastewater, *Chem. Eng. J.*, 2020, 125760.
- 26 H.-P. Cong, *et al.*, Macroscopic multifunctional graphene-based hydrogels and aerogels by a metal ion induced self-assembly process, *ACS Nano*, 2012, **6**(3), 2693–2703.
- 27 S. Zhang, *et al.*, Investigation of the microwave absorbing properties of carbon aerogels, *J. Mater. Sci. Eng. B*, 2002, **90**(1–2), 38–41.
- 28 H.-B. Zhao, *et al.*, Magnetic and conductive Ni/carbon aerogels toward high-performance microwave absorption, *Ind. Eng. Chem. Res.*, 2018, **57**(1), 202–211.
- 29 N. Shah and D. Lin, Composite Aerogels for Biomedical and Environmental Applications, *Curr. Pharm. Des.*, 2020, **26**(45), 5807–5818.
- 30 V. M. Gun'ko, I. N. Savina and S. V. Mikhalovsky, Cryogels: morphological, structural and adsorption characterisation, *Adv. Colloid Interface Sci.*, 2013, **187**, 1–46.
- 31 R. T. Olsson, *et al.*, Making flexible magnetic aerogels and stiff magnetic nanopaper using cellulose nanofibrils as templates, *Nat. Nanotechnol.*, 2010, **5**(8), 584.
- 32 S.-C. Hu, *et al.*, Magnetic mesoporous iron oxide/silica composite aerogels with high adsorption ability for organic pollutant removal, *J. Porous Mater.*, 2016, **23**(3), 655–661.
- 33 J. L. Gurav, *et al.*, Silica aerogel: synthesis and applications, *J. Nanomater.*, 2010, **2010**.
- 34 K. Racka, *et al.*, Magnetic properties of Fe nanoparticle systems, *J. Magn. Magn. Mater.*, 2005, **290**, 127–130.
- 35 S. Taccola, *et al.*, Characterization of free-standing PEDOT: PSS/iron oxide nanoparticle composite thin films and application as conformable humidity sensors, *ACS Appl. Mater. Interfaces*, 2013, **5**(13), 6324–6332.
- 36 R. Du, *et al.*, 3D Self-Supporting Porous Magnetic Assemblies for Water Remediation and Beyond, *Adv. Energy Mater.*, 2016, **6**(17), 1600473.



- 37 E. Zaki, *et al.*, Water Ordering on the Magnetite  $Fe_3O_4$  Surfaces, *J. Phys. Chem. Lett.*, 2019, **10**(10), 2487–2492.
- 38 M. Fronzi and M. Nolan, First-principles analysis of the stability of water on oxidised and reduced  $CuO$  (111) surfaces, *RSC Adv.*, 2017, **7**(89), 56721–56731.
- 39 A. Casu, *et al.*, The influence of composition and porosity on the magnetic properties of  $FeCo-SiO_2$  nanocomposite aerogels, *Phys. Chem. Chem. Phys.*, 2008, **10**(7), 1043–1052.
- 40 D. Carta, *et al.*, Structural and magnetic characterization of Co and Ni silicate hydroxides in bulk and in nanostructures within silica aerogels, *Chem. Mater.*, 2009, **21**(5), 945–953.
- 41 G. Shen, Y. Xu and B. Liu, Preparation and adsorption properties of magnetic mesoporous  $Fe_3C$ /carbon aerogel for arsenic removal from water, *Desalin. Water Treat.*, 2016, **57**(51), 24467–24475.
- 42 D. Xu, *et al.*, Synthesis of magnetic graphene aerogels for microwave absorption by *in situ* pyrolysis, *Carbon*, 2019, **146**, 301–312.
- 43 S. Zhao, *et al.*, Additive manufacturing of silica aerogels, *Nature*, 2020, **584**(7821), 387–392.
- 44 L. Casas, *et al.*, Silica aerogel–iron oxide nanocomposites: structural and magnetic properties, *J. Non-Cryst. Solids*, 2001, **285**(1–3), 37–43.
- 45 Z.-D. Li, *et al.*, Preparation and photocatalytic performance of magnetic  $Fe_3O_4@TiO_2$  core–shell microspheres supported by silica aerogels from industrial fly ash, *J. Alloys Compd.*, 2016, **659**, 240–247.
- 46 J. Wang, *et al.*, A versatile ambient pressure drying approach to synthesize silica-based composite aerogels, *RSC Adv.*, 2014, **4**(93), 51146–51155.
- 47 Y. Li, *et al.*, Programmable Ultralight Magnets via Orientational Arrangement of Ferromagnetic Nanoparticles within Aerogel Hosts, *ACS Nano*, 2019, **13**(12), 13875–13883.
- 48 E.-H. Lee, C.-Y. Kim and Y.-H. Choa, Magnetite nanoparticles dispersed within nanoporous aerogels for hyperthermia application, *Curr. Appl. Phys.*, 2012, **12**, S47–S52.
- 49 L. Amirkhani, J. Moghadas and H. Jafarizadeh-Malmiri, Candida rugosa lipase immobilization on magnetic silica aerogel nanodispersion, *RSC Adv.*, 2016, **6**(15), 12676–12687.
- 50 N. Leventis, *et al.*, Using nanoscopic hosts, magnetic guests, and field alignment to create anisotropic composite gels and aerogels, *Nano Lett.*, 2002, **2**(1), 63–67.
- 51 M. F. van Raap, *et al.*, Detailed magnetic dynamic behaviour of nanocomposite iron oxide aerogels, *J. Phys.: Condens. Matter*, 2005, **17**(41), 6519.
- 52 S. M. Jung, *et al.*, A facile route for 3D aerogels from nanostructured 1D and 2D materials, *Sci. Rep.*, 2012, **2**, 849.
- 53 H. Maleki, *et al.*, Design of multifunctional magnetic hybrid silica aerogels with improved properties, *Microporous Mesoporous Mater.*, 2016, **232**, 227–237.
- 54 S. Nagappan and C.-S. Ha, Emerging trends in superhydrophobic surface based magnetic materials: fabrications and their potential applications, *J. Mater. Chem. A*, 2015, **3**(7), 3224–3251.
- 55 P. M. Zélis, *et al.*, Magnetic hydrophobic nanocomposites: Silica aerogel/maghemite, *Phys. B*, 2012, **407**(16), 3113–3116.
- 56 C. Cannas, *et al.*, Magnetic properties of  $\gamma-Fe_2O_3-SiO_2$  aerogel and xerogel nanocomposite materials, *J. Mater. Chem.*, 2001, **11**(12), 3180–3187.
- 57 M. F. van Raap, *et al.*, Synthesis and magnetic properties of iron oxide–silica aerogel nanocomposites, *Phys. B*, 2007, **398**(2), 229–234.
- 58 F. Luo, *et al.*, Synthesis of paramagnetic iron incorporated silica aerogels by ambient pressure drying, *Mater. Chem. Phys.*, 2013, **142**(1), 113–118.
- 59 M. Popovici, *et al.*, Ultraporous Single Phase Iron Oxide–Silica Nanostructured Aerogels from Ferrous Precursors, *Langmuir*, 2004, **20**(4), 1425–1429.
- 60 L. Casas, *et al.*, Iron oxide nanoparticles hosted in silica aerogels, *Appl. Phys. A*, 2002, **74**(5), 591–597.
- 61 D. Carta, *et al.*, An X-ray absorption spectroscopy study of the inversion degree in zinc ferrite nanocrystals dispersed on a highly porous silica aerogel matrix, *J. Chem. Phys.*, 2013, **138**(5), 054702.
- 62 J. da Silva, *et al.*, Magnetic studies of  $CoFe_2O_4/SiO_2$  aerogel and xerogel nanocomposites, *J. Nanosci. Nanotechnol.*, 2009, **9**(10), 5932–5939.
- 63 D. Carta, *et al.*, Structural study of highly porous nanocomposite aerogels, *J. Non-Cryst. Solids*, 2007, **353**(18–21), 1785–1788.
- 64 D. Carta, *et al.*, Structural characterization study of  $FeCo$  alloy nanoparticles in a highly porous aerogel silica matrix, *J. Chem. Phys.*, 2007, **127**(20), 204705.
- 65 M. F. Casula, A. Corrias and G. Paschina,  $FeCo-SiO_2$  nanocomposite aerogels by high temperature supercritical drying, *J. Mater. Chem.*, 2002, **12**(5), 1505–1510.
- 66 S. Bullita, *et al.*,  $ZnFe_2O_4$  nanoparticles dispersed in a highly porous silica aerogel matrix: a magnetic study, *Phys. Chem. Chem. Phys.*, 2014, **16**(10), 4843–4852.
- 67 A. Lančok, *et al.*, Mössbauer studies on ultraporous  $Fe$ -Oxide/ $SiO_2$  aerogel, in *ICAME 2005*, Springer, 2006, pp. 203–208.
- 68 S. Jones, *et al.*, Thermal calibrations of hypervelocity capture in aerogel using magnetic iron oxide particles, *Icarus*, 2013, **226**(1), 1–9.
- 69 W. Yang, *et al.*, Performance and mass transfer of aqueous fluoride removal by a magnetic alumina aerogel, *RSC Adv.*, 2016, **6**(114), 112988–112999.
- 70 M. F. Casula, *et al.*, Near equiatomic  $FeCo$  nanocrystalline alloy embedded in an alumina aerogel matrix: Microstructural features and related magnetic properties, *J. Phys. Chem. B*, 2005, **109**(50), 23888–23895.
- 71 A. Corrias, *et al.*, Preparation and characterization of  $FeCo-Al_2O_3$  and  $Al_2O_3$  aerogels, *J. Sol-Gel Sci. Technol.*, 2004, **31**(1–3), 83–86.
- 72 Z. Hao, *et al.*, Fluidization characteristics of aerogel  $Co/Al_2O_3$  catalyst in a magnetic fluidized bed and its application to  $CH_4$ – $CO_2$  reforming, *Powder Technol.*, 2008, **183**(1), 46–52.



- 73 S. Zhou, *et al.*, Highly hydrophobic, compressible, and magnetic polystyrene/Fe<sub>3</sub>O<sub>4</sub>/graphene aerogel composite for oil–water separation, *Ind. Eng. Chem. Res.*, 2015, **54**(20), 5460–5467.
- 74 P. Datta, Magnetic gels, in *Polymeric Gels*, Elsevier, 2018, pp. 441–465.
- 75 S. Liu, X. Luo, and J. Zhou, Magnetic responsive cellulose nanocomposites and their applications, in *Cellulose-Medical, Pharmaceutical and Electronic Applications*, IntechOpen, 2013.
- 76 L.-Y. Long, Y.-X. Weng and Y.-Z. Wang, Cellulose aerogels: Synthesis, applications, and prospects, *Polymers*, 2018, **10**(6), 623.
- 77 P. Bober, *et al.*, Conducting polymer composite aerogel with magnetic properties for organic dye removal, *Synth. Met.*, 2020, **260**, 116266.
- 78 K. J. De France, T. Hoare and E. D. Cranston, Review of hydrogels and aerogels containing nanocellulose, *Chem. Mater.*, 2017, **29**(11), 4609–4631.
- 79 H. Gu, *et al.*, Magnetic nanocellulose-magnetite aerogel for easy oil adsorption, *J. Colloid Interface Sci.*, 2020, **560**, 849–856.
- 80 R.-L. Liu, *et al.*, Eco-friendly fabrication of sponge-like magnetically carbonaceous fiber aerogel for high-efficiency oil–water separation, *RSC Adv.*, 2016, **6**(36), 30301–30310.
- 81 S. F. Chin, A. N. B. Romainor and S. C. Pang, Fabrication of hydrophobic and magnetic cellulose aerogel with high oil absorption capacity, *Mater. Lett.*, 2014, **115**, 241–243.
- 82 Y. Jiao, *et al.*, Facile hydrothermal synthesis of Fe<sub>3</sub>O<sub>4</sub>@cellulose aerogel nanocomposite and its application in Fenton-like degradation of Rhodamine B, *Carbohydr. Polym.*, 2018, **189**, 371–378.
- 83 S. Liu, *et al.*, Highly flexible magnetic composite aerogels prepared by using cellulose nanofibril networks as templates, *Carbohydr. Polym.*, 2012, **89**(2), 551–557.
- 84 X. Wang, *et al.*, Magnetic-controlled aerogels from carboxylated cellulose and MnFe<sub>2</sub>O<sub>4</sub> as a novel adsorbent for removal of Cu (II), *Cellulose*, 2019, **26**(8), 5051–5063.
- 85 J. Wei, *et al.*, Nanocellulose-based magnetic hybrid aerogel for adsorption of heavy metal ions from water, *J. Mater. Sci.*, 2019, **54**(8), 6709–6718.
- 86 S. Cui, *et al.*, Preparation of magnetic MnFe<sub>2</sub>O<sub>4</sub>-Cellulose aerogel composite and its kinetics and thermodynamics of Cu (II) adsorption, *Cellulose*, 2018, **25**(1), 735–751.
- 87 K. Srarasi, *et al.*, Recovery potential of cellulose fiber from newspaper waste: An approach on magnetic cellulose aerogel for dye adsorption material, *Int. J. Biol. Macromol.*, 2018, **119**, 662–668.
- 88 Y. Li, *et al.*, Versatile fabrication of magnetic carbon fiber aerogel applied for bidirectional oil–water separation, *Appl. Phys. A*, 2015, **120**(3), 949–957.
- 89 H. Liu, *et al.*, Fabrication of recyclable magnetic double-base aerogel with waste bioresource bagasse as the source of fiber for the enhanced removal of chromium ions from aqueous solution, *Food Bioprod. Process.*, 2020, **119**, 257–267.
- 90 Y. Zhang, *et al.*, Processing cellulose@ Fe<sub>3</sub>O<sub>4</sub> into mechanical, magnetic and biodegradable synapse-like material, *Composites, Part B*, 2019, **177**, 107432.
- 91 C. A. García-González, *et al.*, Design of biocompatible magnetic pectin aerogel monoliths and microspheres, *RSC Adv.*, 2012, **2**(26), 9816–9823.
- 92 C. Wan and J. Li, Synthesis of well-dispersed magnetic CoFe<sub>2</sub>O<sub>4</sub> nanoparticles in cellulose aerogels via a facile oxidative co-precipitation method, *Carbohydr. Polym.*, 2015, **134**, 144–150.
- 93 W. Li, X. Zhao and S. Liu, Preparation of entangled nanocellulose fibers from APMP and its magnetic functional property as matrix, *Carbohydr. Polym.*, 2013, **94**(1), 278–285.
- 94 P. Arabkhani and A. Asfaram, Development of a novel three-dimensional magnetic polymer aerogel as an efficient adsorbent for malachite green removal, *J. Hazard. Mater.*, 2020, **384**, 121394.
- 95 D. Shen, *et al.*, Green synthesis of Fe<sub>3</sub>O<sub>4</sub>/cellulose/polyvinyl alcohol hybride aerogel and its application for dye removal, *J. Polym. Environ.*, 2018, **26**(6), 2234–2242.
- 96 B. Vivek and E. Prasad, Self-Assembly-Directed Aerogel and Membrane Formation from a Magnetic Composite: An Approach to Developing Multifunctional Materials, *ACS Appl. Mater. Interfaces*, 2017, **9**(8), 7619–7628.
- 97 M. M. Abdellatif, *et al.*, Iota-carrageenan based magnetic aerogels as an efficient adsorbent for heavy metals from aqueous solutions, *J. Porous Mater.*, 2020, **27**(1), 277–284.
- 98 Y. Zhang, *et al.*, Synthesis, structure and electromagnetic properties of mesoporous Fe<sub>3</sub>O<sub>4</sub> aerogels by sol-gel method, *J. Mater. Sci. Eng. B*, 2014, **188**, 13–19.
- 99 Y. Li, *et al.*, Multifunctional Organic-Inorganic Hybrid Aerogel for Self-Cleaning, Heat-Insulating, and Highly Efficient Microwave Absorbing Material, *Adv. Funct. Mater.*, 2019, **29**(10), 1807624.
- 100 J.-H. Lee and S.-J. Park, Recent advances in preparations and applications of carbon aerogels: A review, *Carbon*, 2020, **163**, 1–18.
- 101 L. Hu, *et al.*, Carbon aerogel for insulation applications: a review, *Int. J. Thermophys.*, 2019, **40**(4), 39.
- 102 C. Moreno-Castilla and F. Maldonado-Hódar, Carbon aerogels for catalysis applications: An overview, *Carbon*, 2005, **43**(3), 455–465.
- 103 G. Gorgolis and C. Galiotis, Graphene aerogels: a review, *2D Materials*, 2017, **4**(3), 032001.
- 104 J. Dai, *et al.*, 3D macroscopic superhydrophobic magnetic porous carbon aerogel converted from biorenewable popcorn for selective oil–water separation, *Mater. Des.*, 2018, **139**, 122–131.
- 105 Y. Lu, Z. Niu and W. Yuan, Multifunctional magnetic superhydrophobic carbonaceous aerogel with micro/nano-scale hierarchical structures for environmental remediation and energy storage, *Appl. Surf. Sci.*, 2019, **480**, 851–860.



- 106 L. Chen, *et al.*, Bifunctional graphene/γ-Fe<sub>2</sub>O<sub>3</sub> hybrid aerogels with double nanocrystalline networks for enzyme immobilization, *Small*, 2013, **9**(13), 2331–2340.
- 107 M. Yu, *et al.*, Magnetic N-doped carbon aerogel from sodium carboxymethyl cellulose/collagen composite aerogel for dye adsorption and electrochemical supercapacitor, *Int. J. Biol. Macromol.*, 2018, **115**, 185–193.
- 108 S. Ye, *et al.*, KGM-based magnetic carbon aerogels matrix for the uptake of methylene blue and methyl orange, *Int. J. Biol. Macromol.*, 2016, **92**, 1169–1174.
- 109 J. Zhang, *et al.*, Ultralight, compressible and multifunctional carbon aerogels based on natural tubular cellulose, *J. Mater. Chem. A*, 2016, **4**(6), 2069–2074.
- 110 M. Li, *et al.*, Magnetic Fe 3 O 4 carbon aerogel and ionic liquid composite films as an electrochemical interface for accelerated electrochemistry of glucose oxidase and myoglobin, *RSC Adv.*, 2015, **5**(19), 14704–14711.
- 111 N. Chen and Q. Pan, Versatile fabrication of ultralight magnetic foams and application for oil–water separation, *ACS Nano*, 2013, **7**(8), 6875–6883.
- 112 M. Yu, J. Li and L. Wang, Preparation and characterization of magnetic carbon aerogel from pyrolysis of sodium carboxymethyl cellulose aerogel crosslinked by iron trichloride, *J. Porous Mater.*, 2016, **23**(4), 997–1003.
- 113 T. Ahamad, *et al.*, N/S doped highly porous magnetic carbon aerogel derived from sugarcane bagasse cellulose for the removal of bisphenol-A, *Int. J. Biol. Macromol.*, 2019, **132**, 1031–1038.
- 114 Y.-F. Lin and C.-Y. Chang, Magnetic mesoporous iron oxide/carbon aerogel photocatalysts with adsorption ability for organic dye removal, *RSC Adv.*, 2014, **4**(54), 28628–28631.
- 115 K. Tadyszak, *et al.*, Magnetic and electric properties of partially reduced graphene oxide aerogels, *J. Magn. Magn. Mater.*, 2019, **492**, 165656.
- 116 Y. Li, *et al.*, Facile synthesis of Fe<sub>3</sub>O<sub>4</sub> nanoparticles decorated on 3D graphene aerogels as broad-spectrum sorbents for water treatment, *Appl. Surf. Sci.*, 2016, **369**, 11–18.
- 117 Z.-S. Wu, *et al.*, 3D nitrogen-doped graphene aerogel-supported Fe<sub>3</sub>O<sub>4</sub> nanoparticles as efficient electrocatalysts for the oxygen reduction reaction, *J. Am. Chem. Soc.*, 2012, **134**(22), 9082–9085.
- 118 R. Sharma, R. Kotnala and P. Saini, Graphene based porous magnetic aerogel powder for removal of methylene blue from waste water, *J. Environ. & Biotechnol. Res.*, 2017, **6**(1), 146–150.
- 119 N. H. Dang, *et al.*, Preparation of magnetic iron oxide/graphene aerogel nanocomposites for removal of bisphenol A from water, *Synth. Met.*, 2019, **255**, 116106.
- 120 W. Chen, *et al.*, Self-assembly and embedding of nanoparticles by in situ reduced graphene for preparation of a 3D graphene/nanoparticle aerogel, *Adv. Mater.*, 2011, **23**(47), 5679–5683.
- 121 J. Mao, *et al.*, Constructing multifunctional MOF@ rGO hydro/aerogels by the self-assembly process for customized water remediation, *J. Mater. Chem. A*, 2017, **5**(23), 11873–11881.
- 122 X. Jia, *et al.*, Synthesis of lightweight and flexible composite aerogel of mesoporous iron oxide threaded by carbon nanotubes for microwave absorption, *J. Alloys Compd.*, 2017, **697**, 138–146.
- 123 X. Zhang, *et al.*, Dendrimer-linked, renewable and magnetic carbon nanotube aerogels, *Mater. Horiz.*, 2014, **1**(2), 232–236.
- 124 H.-B. Zhao, *et al.*, Ultralight CoNi/rGO aerogels toward excellent microwave absorption at ultrathin thickness, *J. Mater. Chem. C*, 2019, **7**(2), 441–448.
- 125 Y.-F. Lin and J.-L. Chen, Magnetic mesoporous Fe/carbon aerogel structures with enhanced arsenic removal efficiency, *J. Colloid Interface Sci.*, 2014, **420**, 74–79.
- 126 G. Reynolds, *et al.*, Morphological effects on the transport and magnetic properties of polymeric and colloidal carbon aerogels, *Phys. Rev. B*, 1994, **50**(24), 18590.
- 127 E. Carpenter, *et al.*, Magnetic and Mössbauer spectroscopy studies of nanocrystalline iron oxide aerogels, *J. Appl. Phys.*, 2006, **99**(8), 08N711.
- 128 L. El Mir, *et al.*, Optical, electrical and magnetic properties of transparent, n-type conductive Zn<sub>0.90-x</sub>V<sub>0.10Al<sub>x</sub>O</sub> thin films elaborated from aerogel nanoparticles, 2007.
- 129 A. Corrias, *et al.*, Evolution of the structure and magnetic properties of FeCo nanoparticles in an alumina aerogel matrix, *Chem. Mater.*, 2004, **16**(16), 3130–3138.
- 130 H. H. Hamdeh, *et al.*, Magnetic properties of partially-inverted zinc ferrite aerogel powders, *J. Appl. Phys.*, 1997, **81**(4), 1851–1857.
- 131 R. J. Willey, P. Noirclerc and G. Busca, Preparation and characterization of magnesium chromite and magnesium ferrite aerogels, *Chem. Eng. Commun.*, 1993, **123**(1), 1–16.
- 132 R. Shu, *et al.*, Facile synthesis of nitrogen-doped reduced graphene oxide/nickel-zinc ferrite composites as high-performance microwave absorbers in the X-band, *Chem. Eng. J.*, 2020, **384**, 123266.
- 133 J. W. Long, *et al.*, Synthesis and characterization of Mn-FeO<sub>x</sub> aerogels with magnetic properties, *J. Non-Cryst. Solids*, 2004, **350**, 182–188.
- 134 M. Janulevicius, *et al.*, Ultralight Magnetic Nanofibrous GdPO<sub>4</sub> Aerogel, *ACS Omega*, 2020.
- 135 M. Yu, *et al.*, Magnetic carbon aerogel pyrolysis from sodium carboxymethyl cellulose/sodium montmorillonite composite aerogel for removal of organic contamination, *J. Porous Mater.*, 2018, **25**(3), 657–664.
- 136 S. Ye, *et al.*, Development of Mag-FMBO in clay-reinforced KGM aerogels for arsenite removal, *Int. J. Biol. Macromol.*, 2016, **87**, 77–84.
- 137 L. E. Nita, *et al.*, New Trends in Bio-Based Aerogels, *Pharmaceutics*, 2020, **12**(5), 449.
- 138 X. Liu, *et al.*, A Novel Bacterial Cellulose Aerogel Modified with PGMA via ARGET ATRP Method for Catalase Immobilization, *Fibers Polym.*, 2019, **20**(3), 520–526.
- 139 J. Yang, *et al.*, Light-weight and flexible silicone rubber/MWCNTs/Fe3O4 nanocomposite foams for efficient



- electromagnetic interference shielding and microwave absorption, *Compos. Sci. Technol.*, 2019, **181**, 107670.
- 140 H.-B. Zhao, *et al.*, Excellent electromagnetic absorption capability of Ni/carbon based conductive and magnetic foams synthesized via a green one pot route, *ACS Appl. Mater. Interfaces*, 2016, **8**(2), 1468–1477.
- 141 S. Guo, *et al.*, Fe ionic induced strong bioinspired  $\text{Fe}_3\text{O}_4$ @graphene aerogel with excellent electromagnetic shielding effectiveness, *Appl. Surf. Sci.*, 2020, 146569.

